

1-29-2009

Double-interval technique for higher order harmonic generation of a quantum dot mode-locked laser

Furqan Chiragh

Follow this and additional works at: https://digitalrepository.unm.edu/ece_etds

Recommended Citation

Chiragh, Furqan. "Double-interval technique for higher order harmonic generation of a quantum dot mode-locked laser." (2009).
https://digitalrepository.unm.edu/ece_etds/53

This Thesis is brought to you for free and open access by the Engineering ETDs at UNM Digital Repository. It has been accepted for inclusion in Electrical and Computer Engineering ETDs by an authorized administrator of UNM Digital Repository. For more information, please contact disc@unm.edu.

Furqan Latif Chiragh

Candidate

Department of Electrical and Computer Engineering

Department

This thesis is approved, and it is acceptable in quality
and form for publication on microfilm:

Approved by the Thesis Committee:

Prof. Luke F. Lester

, Chairperson

Prof. Christos Christodoulou

Dr. Frédéric Grillot

Accepted:

Dean, Graduate School

Date

**DOUBLE-INTERVAL TECHNIQUE FOR HIGHER ORDER
HARMONIC GENERATION OF A QUANTUM DOT MODE-LOCKED
LASER**

BY

FURQAN LATIF CHIRAGH

B.S. Electrical Engineering, New Mexico Institute of Mining and Technology,
2006

THESIS

Submitted in Partial Fulfillment of the
Requirements for the Degree of

**Master of Science
Electrical Engineering**

The University of New Mexico
Albuquerque, New Mexico

December, 2008

©2008, FURQAN LATIF CHIRAGH

DEDICATION

To my lovely parents Dr. Abdul-Latif Chiragh and Wajahat-un-Nisa Chiragh.

ACKNOWLEDGMENTS

The research for this thesis was carried out at the Center for High Technology Materials (CHTM) at the University of New Mexico. First I would like to thank Allah (SWT) for giving me the guidance and ability to seek knowledge and pursue a master's degree in optoelectronics.

I would like to thank Prof. Luke F. Lester, my advisor and thesis chair, for his direction and leadership in this project. His expertise and ability to teach concepts in the field made my journey pleasurable and enlightening and will remain with me as I continue my career.

I also thank my committee members, Prof. Christos Christodoulou and Dr. Frédéric Grillot, for their valuable recommendations pertaining to this study and assistance in my professional development.

I would like to thank Dr. Yongchun Xin, our post-doctoral student, for his guidance in the laboratory and his eagerness to see me succeed. His efforts helped make this thesis work possible.

I would like to thank my group members for their guidance and assistance. I thank Mohamed El-Emawy, Yan Li, Chang-Yi Lin, Nader Naderi, Mike Pochet, and Therese Saiz for their help in the laboratory and understanding the field.

I would like to thank Omar Qassim, and Yasser Soliman for their help during my graduate studies.

I would also like to thank my sister and brother, Atifa Chiragh and Imran Chiragh. Without their loving care and compassion I would not be where I am today.

Last, but not least, I would like to thank my parents Dr. Abdul-Latif Chiragh and Wajahat-un-Nisa Chiragh. Without their hard work and sacrifices I would not have had the opportunities to enhance my education and achieve what I have. I can never thank you both enough for what you have done for me. I will forever be indebted to you both for all of the difficulties you have endured for me. I love you Abuji and Amiji!

**DOUBLE-INTERVAL TECHNIQUE FOR HIGHER ORDER
HARMONIC GENERATION OF A QUANTUM DOT MODE-LOCKED
LASER**

BY

FURQAN LATIF CHIRAGH

ABSTRACT OF THESIS

Submitted in Partial Fulfillment of the
Requirements for the Degree of

**Master of Science
Electrical Engineering**

The University of New Mexico
Albuquerque, New Mexico

December, 2008

DOUBLE-INTERVAL TECHNIQUE FOR HIGHER ORDER HARMONIC GENERATION OF A QUANTUM DOT MODE-LOCKED LASER

by

Furqan Latif Chiragh

B.S., Electrical Engineering, New Mexico Institute of Mining and Technology, 2006

M.S., Electrical Engineering, University of New Mexico, 2008

ABSTRACT

As the speed barrier is reached in traditional integrated circuits, the need to produce ultra-fast optical pulses is of growing importance. By using optical pulses as clock sequence generators, it is possible to overcome the bottlenecks due to RC delays and the excessive power consumption of today's technology. In this thesis a quantum dot mode-locked laser is passively locked and using the double-interval technique achieves higher order harmonics. The double-interval technique is commonly used with musicians to create false harmonics while they strum their instruments. When a violinist places his finger upon a string he creates a node that changes the tune of the violin as it is strummed. The strumming of the violin without the violinist placing a finger upon the fingerboard creates the first harmonic also known as the fundamental harmonic. If the location of the node were in the center of the fingerboard, this would result in the creation of the second harmonic. Placing the finger at a location at a third, fourth, or fifth of the fingerboard will result with the third, fourth, and fifth harmonics, respectively. Using this as a base the double-interval technique is applied to a passively locked mode-locked laser

in this study. The double-interval technique allows for the generation of harmonics that would not easily be possible with a traditional passively locked mode-locked laser. The double-interval technique utilizes the stimulation of the prime number harmonics in unison in order to achieve higher order harmonics. The laser in this study has a fundamental frequency of approximately 6.0 GHz and its second, third, fifth, sixth, and tenth harmonics are presented.

TABLE OF CONTENTS

LIST OF FIGURES	XII
LIST OF TABLES	XVI
CHAPTER 1 - INTRODUCTION.....	1
1.1 Overview of Laser Technology	1
1.2 Laser Mode-Locking	2
1.2.1 Active Mode Locking.....	3
1.2.2 Passive Mode-Locking	6
1.2.3 Colliding Pulse Mode-Locking	8
1.3 Double-Interval Harmonic Mode-Locking	9
1.4 Organization of Thesis	11
CHAPTER 2 - THEORY AND MEASUREMENT PROCESS	13
2.1 Colliding Pulse Technique for Higher Order Harmonic Generation.....	13
2.2 Predictive Model Using the Colliding Pulse Equation.....	15
2.3 Device Design and Fabrication	20
2.4 Measurement Setup	27
CHAPTER 3 - DATA AND MEASUREMENTS	32
3.1 Rationalization and Focus of the Experiment.....	32
3.1.1 Fundamental Harmonic Laser Characteristics.....	32
3.1.2 Second Harmonic Laser Characteristics	36
3.1.3 Third Harmonic Laser Characteristics.....	41
3.1.4 Fifth Harmonic Laser Characteristics	47
3.2 Double-Interval Experimentation	52
3.2.1 Sixth Harmonic Laser Characteristics.....	53

3.2.2 Tenth Harmonic Laser Characteristics	58
3.3 <i>Analysis</i>	62
CHAPTER 4 - SUMMARY AND FUTURE WORK	64
4.1 <i>Summary</i>	64
4.2 <i>Future Work</i>	65
REFERENCES.....	67

LIST OF FIGURES

Figure 1-1 The creation of pulses using the internal gain and loss of a laser [8].....	3
Figure 1-2 Generation of optical pulses by active mode-locking [11].....	4
Figure 1-3 An example of an actively mode-locked laser employing an acousto-optic- modulator (AOM) [8]	5
Figure 1-4 An example of a passively mode-locked laser with a slow saturable absorber [12].....	7
Figure 1-5 An example of a passively mode-locked laser with a fast saturable absorber [12].....	7
Figure 1-6 Schematic of a monolithic CPM laser [17]	9
Figure 1-7 Comparison between device segmentation for double-interval mode-locking and traditional mode-locking for the 10 th harmonic of a laser diode	11
Figure 2-1 Location of nodes and corresponding harmonic generated [21]	14
Figure 2-2 Laser anti-nodes for creation of tenth harmonic.....	15
Figure 2-3 50 GHz span of the mode-locked laser's fundamental harmonic (6.0 GHz), 2 nd harmonic (12.0 GHz), 3 rd harmonic (18.0 GHz), 5 th harmonic (30.0 GHz), and 6 th harmonic (36.0 GHz)	16
Figure 2-4 Model of optical intensities needed to create the second harmonic	18
Figure 2-5 Zia Wafer 1023 growth structure	21
Figure 2-6 Standard processing for standard segmented contact devices [32]	24
Figure 2-7 Segmented device.....	25
Figure 2-8 The 250- μ m and 500- μ m contact-pad AlN substrates	26
Figure 2-9 Wirebonding of the 250- μ m anodes.....	26

Figure 2-10 Side view of the copper stage with the TEC	27
Figure 2-11 Probe card connected to device	28
Figure 2-12 Reconfigurable board for biasing the laser.....	29
Figure 2-13 Complete system schematic	31
Figure 3-1 Configuration for the generation of the fundamental harmonic	34
Figure 3-2 50 GHz span of the laser diode's fundamental repetition rate	35
Figure 3-3 100 MHz span of the fundamental repetition rate.....	35
Figure 3-4 Pulse width associated with the fundamental harmonic repetition rate	36
Figure 3-5 Configuration for the generation of the second harmonic using three saturable absorbers	37
Figure 3-6 Pulse width associated with the second harmonic repetition rate for when three sections of saturable absorber is used	38
Figure 3-7 Configuration for the generation of the second harmonic.....	39
Figure 3-8 50 GHz span of repetition rate while configured for second harmonic generation.....	40
Figure 3-9 100 MHz span of the second harmonic repetition rate.....	40
Figure 3-10 Pulse width associated with the second harmonic repetition rate	41
Figure 3-11 Possible configurations for the generation of the third harmonic. (a) Using only sections 9&10, (b) using only sections 18&19, and (c) using sections 9&10 and 19&18.....	43
Figure 3-12 Configuration for the generation of the third harmonic	45
Figure 3-13 50 GHz span of repetition rate while configured for third harmonic generation.....	45

Figure 3-14 100 MHz span of the third harmonic repetition rate	46
Figure 3-15 Pulse width associated with the third harmonic repetition rate.....	46
Figure 3-16 Possible configuration for the generation of the fifth harmonic. (a) Using only section 6, (b) using only section 22, and (c) using section 6 and 22.....	48
Figure 3-17 Configuration for the generation of the fifth harmonic	50
Figure 3-18 50 GHz span of repetition rate while configured for fifth harmonic generation.....	50
Figure 3-19 100 MHz span of the fifth harmonic repetition rate.....	51
Figure 3-20 Pulse width associated with the fifth harmonic repetition rate	51
Figure 3-21 Possible configuration for the generation of the sixth harmonic. (a) Using the traditional method and placing a saturable absorber at either section 5 or 23, (b) using both sections 5 and 23, (c) using the double-interval technique by placing saturable absorbers at section 14 and 18&19, and (d) using the double-interval technique by placing saturable absorbers at section 14 and 9&10 and 18&19.....	54
Figure 3-22 Double interval configuration for the generation of the sixth harmonic.....	56
Figure 3-23 50 GHz Span of repetition rate while configured for sixth harmonic generation.....	56
Figure 3-24 100 MHz span of the sixth harmonic repetition rate.....	57
Figure 3-25 Pulse width associated with the sixth harmonic repetition rate	57
Figure 3-26 Possible configuration for the generation of the tenth harmonic. (a) Using the traditional method and placing a saturable absorber at either section 3 or 25, (b) using both sections 3 and 25, (c) using the double-interval technique by placing	

saturable absorbers at section 14 and 22, and (d) using the double-interval technique by placing saturable absorbers at section 14 and 6 and 22.....	59
Figure 3-27 Double interval configuration for the generation of the tenth harmonic.....	61
Figure 3-28 50 GHz span of repetition rate while configured for tenth harmonic generation.....	61
Figure 3-29 Pulse width associated with the tenth harmonic repetition rate	62

LIST OF TABLES

Table 3-1 Comparison of expected values for the repetition rates and the measured values for the repetition rates for the harmonics generated	63
Table 3-2 Comparison between pulse widths and stimulated harmonics	63

CHAPTER 1 - INTRODUCTION

1.1 Overview of Laser Technology

With the world's escalating thirst for knowledge, traditional means of communication will soon be insufficient to meet the market's growing demand. It is foreseen that since silicon CMOS features are shrinking, bottlenecks due to RC delays are occurring, and with power consumption of integrated circuits rapidly rising [1, 2], laser technology is the solution. That is why since data communications revolutionized in the late 20th Century, scientists have moved towards optical communications because of its extremely fast speed, the speed of light. The invention of more monochromatic and monolithic semiconductor lasers has set the stage for faster communications. Since semiconductor lasers are small in size and easy to operate by means of electrical pumping, they can provide the necessary modulation capability required for high-speed communications [3-7]. By controlling the operating conditions of the laser, it is possible to create ultra-fast pulses of light. These optical pulses can be used in a wide range of applications such as local oscillator sources for millimeter-wave imaging, radio astronomy, atmospheric sensing, and clock sequence generators in optical communications [6]. One of the best techniques for creating these optical pulses is mode locking in a laser diode.

Using a mode-locked laser, the objective of this thesis is to investigate the so-called "double-interval technique" with application to higher order harmonic generation in the device. This is advantageous because the double-interval technique allows for the

generation of harmonics that would not easily be possible in conventional semiconductor mode-locked lasers.

1.2 Laser Mode-Locking

The task of mode-locking is to get as many of the laser's longitudinal modes to operate in a phase synchronous fashion, such that the superposition of all modes represents a pulse with a spatial extent much shorter than the cavity [8]. In essence it allows all of the laser's optical power to be confined into a very small region rather than across the entire laser cavity. By doing this, mode-locking allows for the generation of ultra fast pulses with smaller pulse widths compared to a traditional laser. The most prominent methods are active mode-locking, passive mode-locking, and colliding pulse mode-locking. Figure 1-1 shows an example of the generation of optical pulses confined to a small region by the saturable absorber of the laser. The blue sections are either mirrors or cleaved facets that create the desired laser cavity length. T_R is the roundtrip time needed for a pulse to pass through the system. The bottom half of Figure 1-1 shows the generation of optical pulses. This occurs when the gain becomes larger than the loss resulting in positive net gain. The necessity of the saturable absorber will be discussed in the following sections. Mode-locking of semiconductor lasers can be realized using many different techniques.

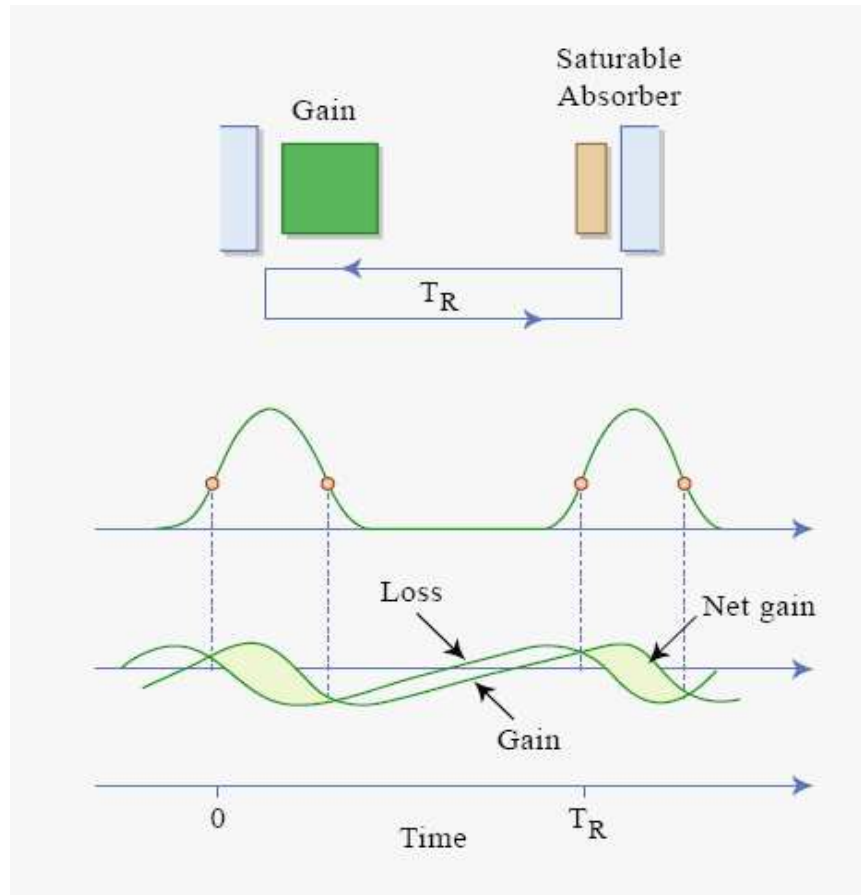


Figure 1-1 The creation of pulses using the internal gain and loss of a laser [8]

1.2.1 Active Mode Locking

Active mode-locking is used to create laser spectra that are no longer randomly fluctuating, but rather controllable by operating conditions [9]. Typically, active mode-locking utilizes external sources to modulate the gain and/or loss in the laser. As seen in Figure 1-2, an optical pulse is emitted when the gain of the laser is greater than its losses. The creation of the pulses can be regulated by actively pumping light into the laser by optical modulators or by controlling the loss in the laser with a Radio Frequency (RF) source. By controlling the amount of loss or gain in a certain region of the laser, it is possible to make the laser pulse at a desired frequency. The modulation of the loss region

is reminiscent of an on/off switch for the optical pulses. Furthermore, the frequency used to control the gain or loss of the laser is also equal to the intermodal spacing of the optical output [10]. The intermodal spacing, $\delta\nu$, is directly related to the driving current frequency by the relation $\delta\nu = \frac{1}{T}$ where T is the period of the driving current's modulation. The best condition for active mode-locking is achieved when T is exactly equal to the round-trip time of the laser's cavity. Generally this will result with an intermodal spacing in the range of 0.3 and 20 GHz. This distinguishes active mode-locking from gain-switched lasers where the pulse frequency is not related to the cavity length of the laser. Fundamentally when the loss is less than the gain it creates an optical window that allows the optical pulse to exit the system and emit from the laser. An example of an actively mode-locked laser is shown in Figure 1-3 where the laser feeds into an Acousto-Optic-Modulator (AOM), which behaves as the optical window for the pulses.

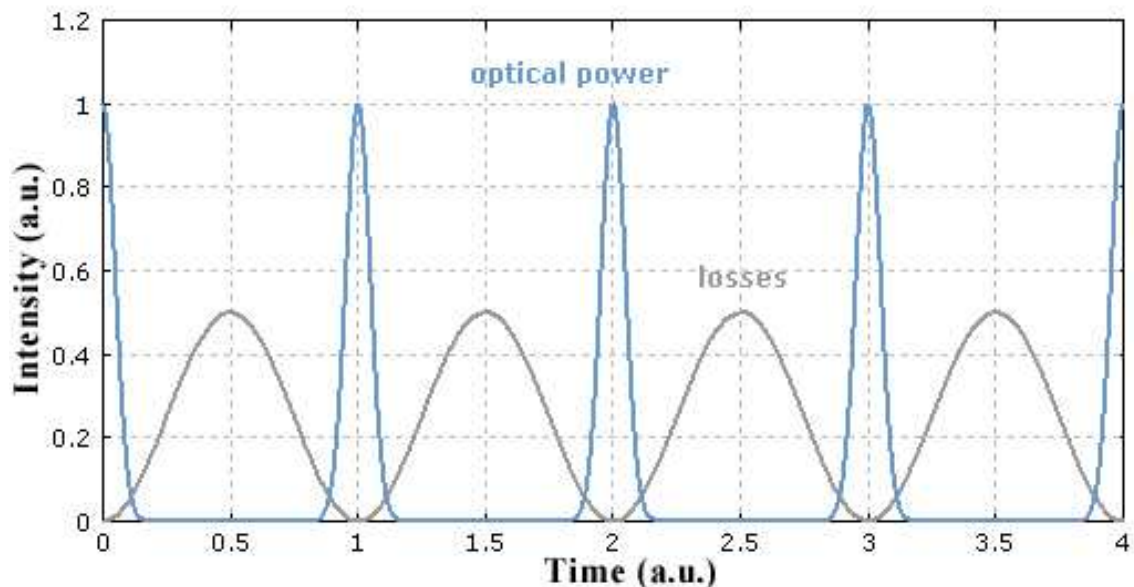


Figure 1-2 Generation of optical pulses by active mode-locking [11]

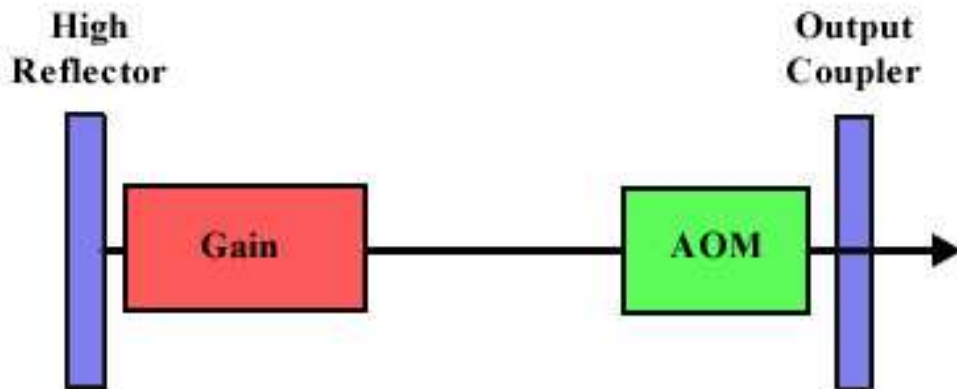


Figure 1-3 An example of an actively mode-locked laser employing an acousto-optic-modulator (AOM) [8]

Active mode-locking is difficult to control because of all of the variables involved. These variables include the placement of a standing wave acousto-optic modulator inside the laser cavity, the placement of a modulation device inside the laser cavity to induce a frequency shift based upon electro-optic effects, and/or the modulation of the energy source pumping the laser itself. When using external optical sources, free space optics makes coupling into the laser difficult and optical modulators also reduce efficiency. Losses make it difficult to control the mode-locking due to the presence of such a weak signal. Another major disadvantage of the active mode-locking technique is its dependence on the external modulation rate [8]. The pulse rate is limited to the speed of the signal generator and cannot surpass it. In order to create pulses faster than the electronic signal generator, the laser needs to be configured in such a way that it can generate the desired pulses on its own. A design that creates a self-pulsating laser within

a self-contained system without the use of external optics is the passive mode-locking configuration of a laser diode.

1.2.2 Passive Mode-Locking

Passive mode-locking harnesses the time dependences of the gain and loss saturation energies to create the desired pulses. By creating very small regions where the laser's gain is greater than its losses, ultra-fast pulses can be produced. When the losses in a laser are greater than the gain, it would appear as if the laser is off. This is because there is not enough energy to create the stimulated emission required for lasing. It is said that the net gain is zero because there is no positive gain. It is very important that as the loss and gain approach their steady-state values, that the loss remains larger than the gain in the regions where pulse generation is not desired. Once the gain is slightly greater than the losses, resulting in net gain, there will be enough energy to cause the laser to turn on and emit light. The key to creating pulses in the passive mode-locked laser is to control the region in which there is net gain. Implementing a saturable absorber into the system can control the amount of loss as a function of power such that the peak of the pulse that has spontaneously formed will see very little loss relative to the wings of the pulse. The saturable absorber is a region in the laser diode where the amount of loss can be controlled by controlling the reverse bias applied. The main purpose of the saturable absorber is to create a region in which the pulse will be shaped. This region will be able to pull in the wings of the broad pulse and create a thinner pulse while maintaining the same average power. If the recovery time of the saturable absorber is much longer with respect to the duration of the pulses then it is called a slow absorber [8]. Otherwise, the

absorber is commonly referred to as a fast absorber [10, 13]. Figure 1-4 and Figure 1-5 show the generation of an optical pulse while displaying the gain and loss saturation energies for a slow and fast absorber, respectively.

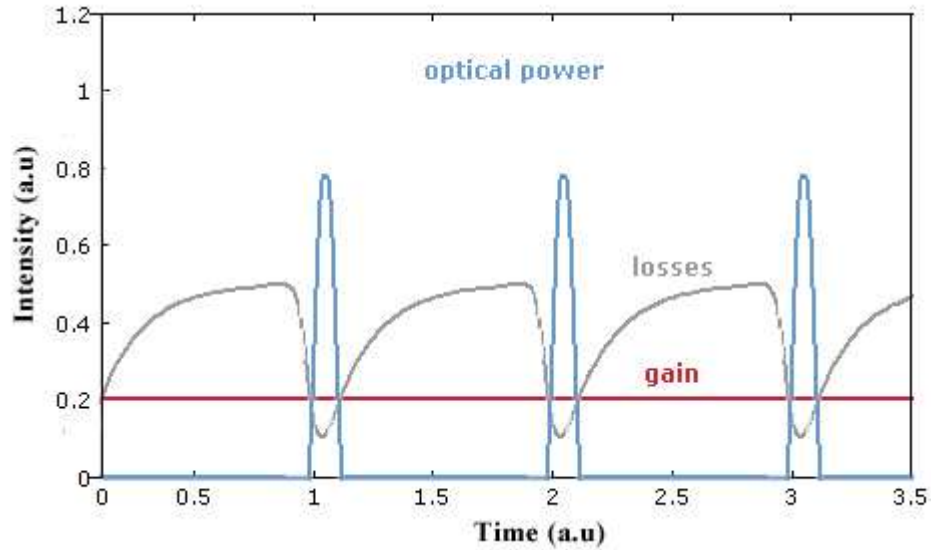


Figure 1-4 An example of a passively mode-locked laser with a slow saturable absorber [12]

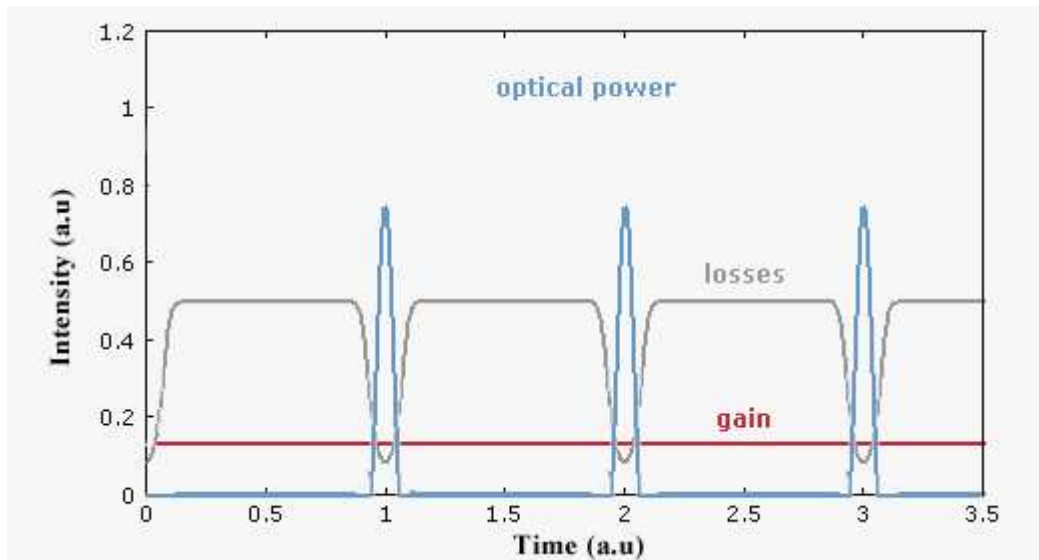


Figure 1-5 An example of a passively mode-locked laser with a fast saturable absorber [12]

1.2.3 Colliding Pulse Mode-Locking

The colliding pulse mode-locking technique (CPM) has been shown to be very effective in creating optical pulses that are in the femtosecond range [14, 15]. CPM utilizes the forward and backwards traveling light inside the laser cavity to build up a transient standing wave. An example of a monolithic CPM laser is shown in Figure 1-6. The ultra-short pulses are achieved by having these forward- and backward-traveling waves collide inside the absorber section and saturating (bleaching) the section. This collision creates a spike in optical intensity creating an associated pulse. The collision creates a much stronger saturation of the absorber than would be possible with just a single pulse traveling through at one time. The length of the absorber section can control the ease and quality of mode locking. The absorber introduces a nonlinearity that leads to a change in pulse shape, which causes the pulse to compress [10]. If the colliding pulses traveling into the absorber section are relatively large compared to the absorber, the resultant pulse will undergo significant compression due to the short length of the absorber section. This pulse will not only have significant compression, but it will be near the saturation energy of the gain section. The energy associated with the wide pulse is conserved, but is now confined into a smaller pulse width, which results in a greater intensity. This is a very important aspect to CPM because it allows passively mode-locked laser to operate at low pulse energy for maximum compression [3] while still providing adequate optical power. It is also possible to apply this technique in order to generate higher order harmonics of the laser's fundamental frequency.

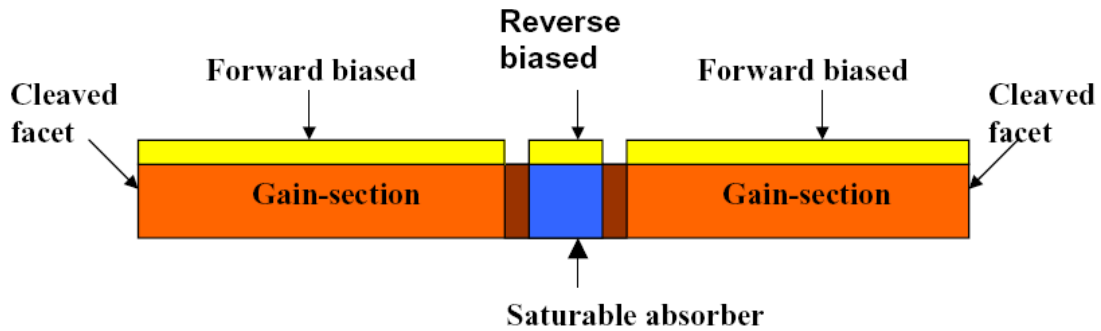


Figure 1-6 Schematic of a monolithic CPM laser [17]

1.3 Double-Interval Harmonic Mode-Locking

Double-interval mode-locking takes advantage of a semiconductor laser's ease of reconfigurability and harmonic mode-locking. The double interval technique refers to using two saturable absorbers that independently stimulate harmonics of the device in order to achieve the multiplicative value of the two harmonics. The double interval technique is similar to CPM in that it utilizes saturable absorbers to create a pulse. The unique aspect of the double-interval technique is that by creating two saturable absorber sections within the laser cavity, it is possible to create a condition where the pulses created can collide together and affect each other. By using this knowledge, it is possible to place the absorbers in specific locations in order to create the desired optical pulse. For example, to stimulate the laser's tenth harmonic a saturable absorber can be placed in the midpoint of the laser diode and another at a point corresponding to a fifth of the laser diode. Individually they would stimulate the second and fifth harmonics, but with the double-interval technique they are stimulated simultaneously and result in the stimulation of the tenth harmonic. A harmonically mode-locked laser produces an optical pulse train

at a multiple of the fundamental round-trip frequency [16]. This is very advantageous for semiconductor lasers because they already have a high fundamental frequency due to their short cavity length. Combined with the double interval technique it is possible to get very high repetition rates from semiconductor laser diodes. Photolithography techniques and mask designs can create a segmented semiconductor laser diode, but as more and more divisions are desired it becomes difficult to achieve good results. Double interval harmonic mode-locking is beneficial because it overcomes the limitations introduced by standard processing. By utilizing this technique it is possible to lock to higher order harmonics that would correspond to repetition rates that would be very difficult to achieve by just mode-locking alone. As seen in Figure 1-7 it is possible to segment the device for the double-interval technique or into divisions that will allow for the simulation of the desired harmonic. In the case for Figure 1-7, it is desired to stimulate the 10th harmonic of the device. Traditionally this would require the device to be segmented in order to isolate a section that would correspond to a tenth of the device. As discussed earlier this may be limited to photolithography techniques and as dimensions get smaller it becomes difficult to wire-bond and probe the device. With the double-interval technique it is possible to maintain larger segments and stimulate the 10th harmonic.

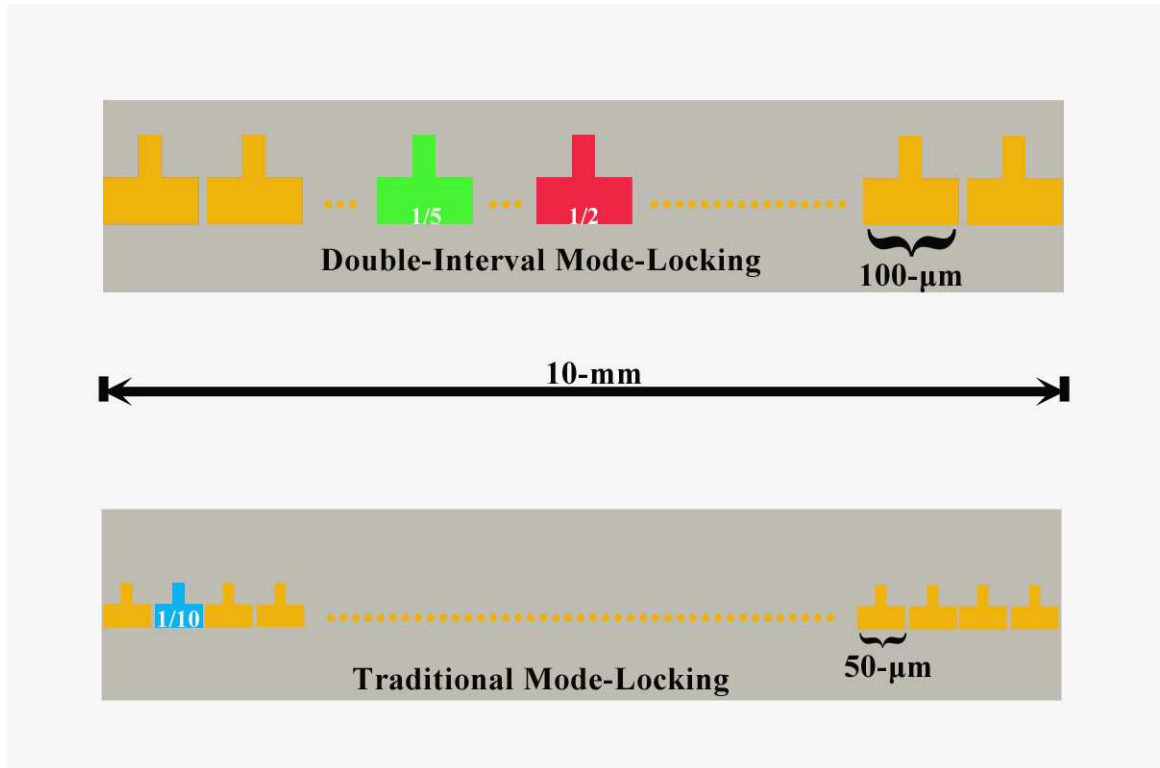


Figure 1-7 Comparison between device segmentation for double-interval mode-locking and traditional mode-locking for the 10th harmonic of a laser diode

The goal of this thesis is to see if it is possible to stimulate higher order harmonics of the mode-locked laser utilizing the double interval technique exploited by violinists. This thesis will apply the double interval technique to a semiconductor laser by using the device's geometry and multiple absorber sections in order to stimulate higher order harmonics.

1.4 Organization of Thesis

Chapter 2 will discuss in detail how the double interval harmonic mode-locking technique is used to achieve the generation of the 2nd, 3rd, 5th, 6th, and 10th harmonics of a Gallium Arsenide Quantum Dot semiconductor laser with a fundamental frequency of approximately 6.0 GHz. A predictive equation first formulated by Yongchun Xin used to

optimize performance will be discussed as well. The experimental setup will also be introduced and explained. Chapter 3 will discuss the results obtained by the experiments. Chapter 4 will discuss conclusions from this experimental effort and will describe possible avenues for future work.

CHAPTER 2 - THEORY AND MEASUREMENT PROCESS

2.1 Colliding Pulse Technique for Higher Order Harmonic Generation

The double-interval technique utilizes colliding pulses to generate higher order harmonics of a semiconductor laser diode. Using the colliding pulse technique, higher order harmonics of the repetition rate can be excited [18, 19]. This knowledge coupled with a musician's ability to generate artificial harmonics sets the stage for this thesis. Analogous to the method used by a violinist to create high order harmonic sounds, the colliding pulse technique can create higher order harmonics of a laser's fundamental frequency. The difference is with the mode-locked laser anti-nodes are created rather than nodes. When a violinist places his finger upon a string he creates a node that changes the tune of the violin as it is strummed. The strumming of the violin without the violinist placing a finger upon the fingerboard creates the first harmonic also known as the fundamental harmonic. If the location of the node were in the center of the fingerboard, this would result in the creation of the second harmonic. Placing the finger at a location at a third, fourth, or fifth of the fingerboard will result with the third, fourth, and fifth harmonics, respectively. Figure 2-1 shows the locations of nodes and the corresponding harmonics.

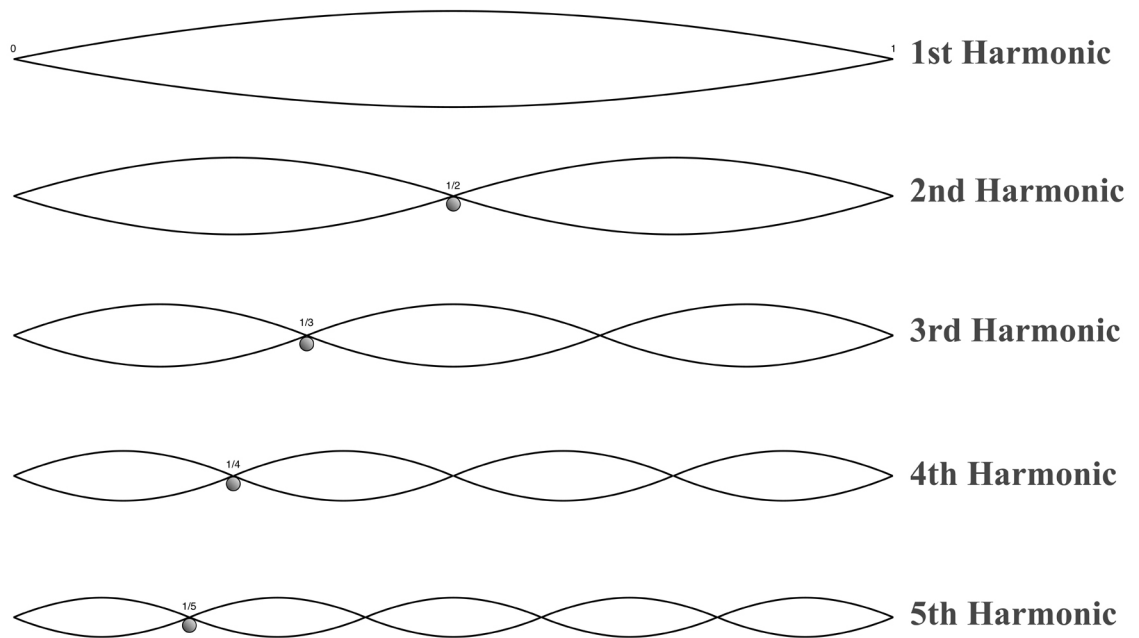


Figure 2-1 Location of nodes and corresponding harmonic generated [21]

By stimulating multiple nodes simultaneously, it is possible to create higher order harmonics that are equivalent to the product of the nodes' harmonics. Since it is possible to create the second and fifth harmonics separately, applying both nodes concurrently will create the tenth harmonic. This technique is applied to the device in this experiment to create the higher order harmonics of the laser's fundamental repetition rate.

When applied to a mode-locked laser technique, applying a reverse bias to the corresponding location creates an absorber section. If this absorber is saturable, not strong enough to absorb all of the excess carriers present, then it behaves as an anti-node. This saturable absorber is an anti-node because it creates a location where a maximum can occur rather than a fixed minimum as with a node. It is these anti-nodes that are needed to provide the generation of the higher order harmonics. Also, obtaining high order harmonics would be difficult to achieve by simply creating a single anti-node. This

would require placing the anti-node at a division of the laser that might be impractical to achieve. Thus multiple anti-nodes can be used to generate the desired harmonic using the double-interval technique. Figure 2-2 shows an example of a laser diode with anti-nodes corresponding to the second and fifth harmonics which are used to create the tenth harmonic. This allows for the generation of harmonics that would not be possible to create with just one anti-node. With this device in particular, when the saturable absorber was placed close to the sections corresponding to the fundamental repetition rate, the fundamental repetition rate was excited. So to stimulate the tenth harmonic with just one saturable absorber at the location corresponding to 25 in Figure 2-2 was not possible because it stimulated the fundamental harmonic.

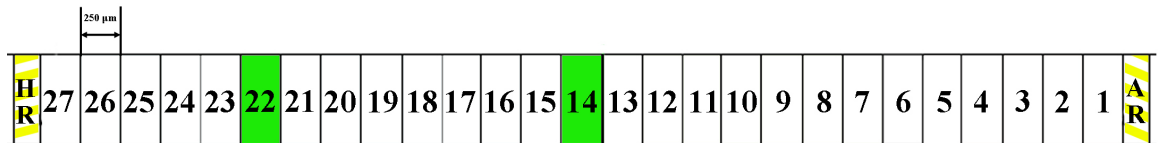


Figure 2-2 Laser anti-nodes for creation of tenth harmonic

2.2 Predictive Model Using the Colliding Pulse Equation

A large amount of both theoretical and experimental research has been performed on semiconductor quantum well and quantum dot passive mode-locked lasers [20, 22-28]. From these studies it is clear that there are many variables that can be altered in order to reach a result such as adjusting the amount of gain in the device, the type of absorber section(s), and the location of the absorber section(s). That is why the predictive model first proposed by Y. C. Xin is of great importance. It utilizes knowledge of semiconductor gain/loss characteristics to maximize the cavity photon density in region(s) that will accentuate particular harmonics of the mode-locked RF spectrum.

Figure 2-3 shows the Radio Frequency (RF) spectrum for the fundamental, 2nd, 3rd, 5th, and 6th harmonics of the mode-locked laser.

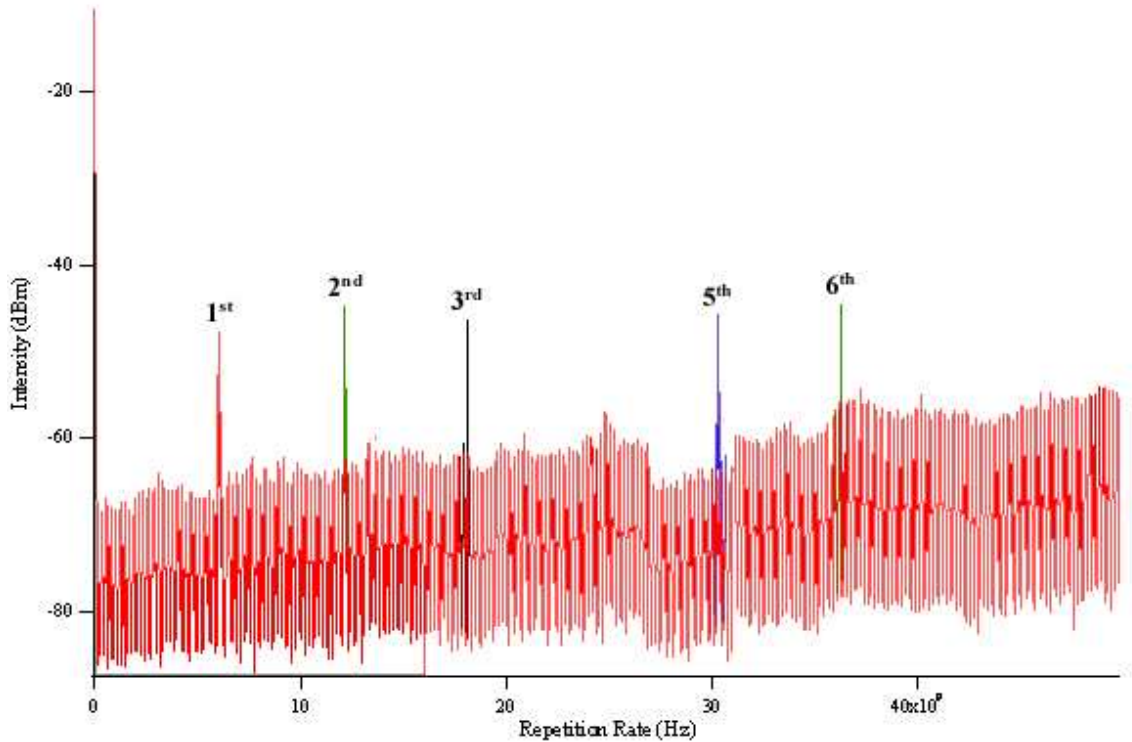


Figure 2-3 50 GHz span of the mode-locked laser’s fundamental harmonic (6.0 GHz), 2nd harmonic (12.0 GHz), 3rd harmonic (18.0 GHz), 5th harmonic (30.0 GHz), and 6th harmonic (36.0 GHz)

Since it is desired to have the pulses collide inside the saturable absorber, the forward and backwards traveling waves must be of enough combined intensity in order to saturate the absorber. As stated earlier, in order to generate optical pulses for a passive mode-locked laser the loss must saturate faster than the gain. This introduces the stability condition s of a passively mode-locked laser, Eqn. 2-1. The stability condition gauges the quality of the laser’s mode-locking and is used as a guideline for getting into the locking regime.

$$s = \frac{E_{sat,g}}{E_{sat,abs}} = \frac{h\nu A_m / \Gamma dg/dN}{n_{tr} h\nu A_m} = \frac{1}{n_{tr} \Gamma \frac{dg}{dN}} = \frac{2}{n_{QD} \Gamma G_g} \quad \text{Eqn. 2-1}$$

Where $E_{sat,abs}$ is the saturation energy of the absorber and $E_{sat,g}$ is the saturation energy of the gain section. Additionally, h is Planck's constant, ν is the optical frequency, A_m is the mode cross-sectional area, Γ is the confinement factor, dg/dN is the differential gain with respect to carrier density, and n_{tr} is the transparency density. It is desirable to have an s greater than 1 to keep the laser in the stable passive mode-locking regime. This implies that for stable CPM operation it is desired to have small differential gain, confinement factor, and dot density.

The intensity of a pulse in the CPM is of great importance. The pulse intensity is usually studied by looking into the amplified spontaneous emission (ASE) of the pulse. The ASE intensity, I , of a propagating pulse moving in the positive x-direction is a function of the net modal gain, G , and the signal testing position, x [29, 30]:

$$\begin{aligned} \frac{dI}{dx} &= G \cdot I + S \\ G &= \Gamma \cdot G_m - \alpha_i \end{aligned} \quad \text{Eqn. 2-2}$$

Where the S is the intensity of the spontaneous emission emitted in all directions, Γ is the optical confinement factor, G_m is the material gain and α_i is the internal loss.

After solving this equation it is possible to find I after it has propagated a total length of L :

$$\ln\left(I + \frac{S}{G}\right) - \ln\left(I_0 + \frac{S}{G}\right) = G \cdot L \quad \text{Eqn. 2-3}$$

Where I_0 is the intensity of the signal at the starting point. For the single pass case we obtain the solution as [31]:

$$I = \frac{S}{G} \left(e^{G \cdot L} - 1 \right) \quad \text{Eqn. 2-4}$$

Using this equation and setting some of the variables as constants, it is possible to find the operating conditions in order to achieve higher harmonics.

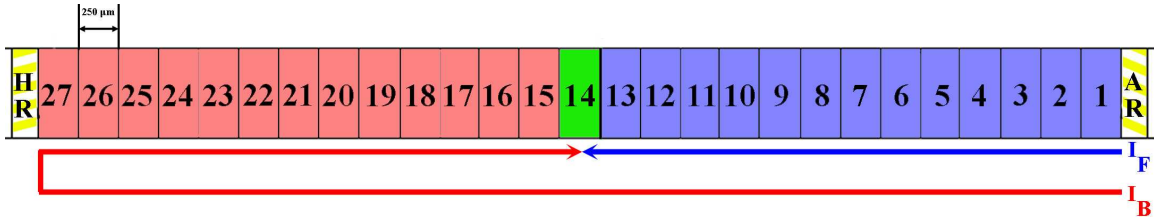


Figure 2-4 Model of optical intensities needed to create the second harmonic

It is desired to have the forward and backward-traveling pulses collide inside the saturable absorber because this will allow the desired harmonic to be stimulated. For the generation of the 2nd harmonic, the saturable absorber needs to be located in the center of the laser diode, as indicated by the green section in Figure 2-4. For simplicity, let us first study the forward traveling pulse, which we choose to have originate at the Anti-Reflectivity Coating (ARC) facet and propagate towards the High Reflectivity Coating (HRC) facet. The purpose for applying the ARC and HRC to the laser's facets is to create

a gain cavity where we control the emittance to just one facet, the ARC side. The pulse travels through the first gain region shown in light blue. As it travels through this region it is amplified by the gain of the first region, G_1 , and the length, L_1 . Since it is desired to have the pulses collide in the middle of the absorber, the pulse will also undergo some time-averaged loss due to the absorber. This time-averaged loss will allow the optical pulse to be trimmed/narrowed and appear to be more Gaussian like. The distance it will travel inside the absorber, half of the absorber length, will be $l_{a/2}$. The resultant equation for the forward traveling pulse (I_F) is

$$I_F = \frac{S}{G_1} \left(e^{G_1 \cdot L_1} - 1 \right) e^{-\alpha \cdot \frac{l_a}{2}} \quad \text{Eqn 2-5}$$

Where S is the spontaneous energy, G_1 and L_1 are the gain and length associated with the blue region in Figure 2-4, α is the loss associated with the absorber, and $l_{a/2}$ is half the length of the absorber section.

To get the backwards traveling wave (I_B) we must continue the journey of the pulse from the forward traveling wave until it reflects off of the HRC facet and returns to the midpoint of the absorber. If there is a previous optical intensity, as with this case, the following equation can be used.

$$I = \left(I_0 + \frac{S}{G} \right) \cdot e^{G \cdot x} \quad \text{Eqn 2-6}$$

Eqn 2-6 is a general equation for resultant intensity when an initial optical intensity is present. Where x is the length traveled through a gain region and I_0 is the previous optical

intensity. Using this generalized equation we can continue the journey of I_F . The pulse will now undergo the remaining average loss of the absorber section and travel through the second gain section, with length L_2 and gain of G_2 as indicated by the light red colored section in Figure 2-4. It should be noted that the reason there is L_1 & L_2 and G_1 & G_2 is because the lengths and gain values could vary depending upon the location of the saturable absorber and the pumping current. After reflecting off of the HRC facet the pulse will travel through a length L_2 and G_2 . Then the pulse will encounter some loss again as it travels to the mid-point of the saturable absorber. The resultant equation for the backwards traveling pulse, as shown in Figure 2-4, is

$$I_B = \left[\left[\frac{S}{G_1} \cdot (e^{G_1 \cdot L_1} - 1) \cdot e^{-\alpha \cdot l_a} + \frac{S}{G_2} \right] \cdot e^{2 \cdot G_2 \cdot L_2} - \frac{S}{G_2} \right] \cdot e^{-\alpha \cdot \frac{l_a}{2}} \quad \text{Eqn 2-7}$$

Where l_a is the total absorber length, $l_{a/2}$ is half the length of the absorber section, and l_c is the total cavity length. The sum of I_F and I_B is the round trip of a single pulse through the entire laser cavity, but it is broken up into the I_F and I_B to study the pulses colliding inside the saturable absorber. It is desired to have the pulses collide as close to the middle of the absorber section to ensure that the pulse trimming that occurs is as symmetric as possible.

2.3 Device Design and Fabrication

This experiment was carried out on devices fabricated on a wafer produced by Zia Laser, Inc. The wafer was ZLG1023 which was grown upon a GaAs substrate material using Molecular Beam Epitaxy (MBE). It has 10 stacks of InAs-InGaAs dots-in-a-well

(DWELL) layers in the active region with GaAs barriers. The cladding layers are $\text{Al}_{0.66}\text{Ga}_{0.34}\text{As}$ and the GaAs barriers layers above the dot layers are un-doped with 60 holes per dot. Figure 2-5 shows the growth structure for ZLG 1023.

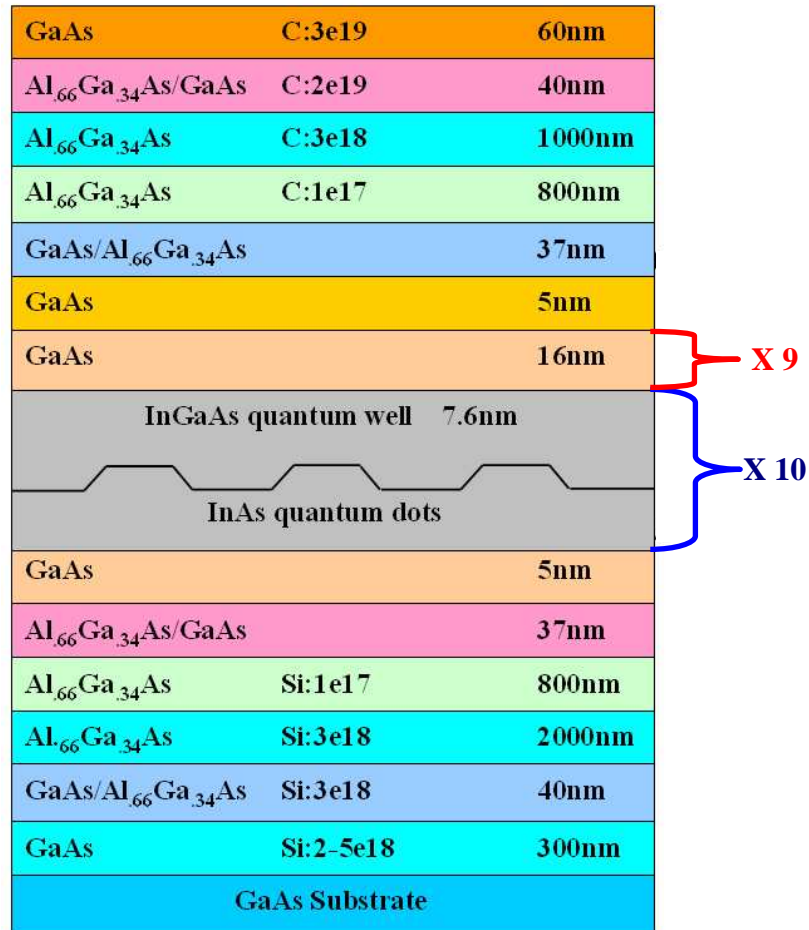


Figure 2-5 Zia Wafer 1023 growth structure

After the growth process, the wafer was taken into the cleanroom to undergo standard waveguide processing. The wafer was cleaned with a 1:30 ammonium hydroxide solution to remove any native oxide that may have formed between growth and processing. This was done to ensure that the following steps would be completed properly. Following the native oxide etch, the wafer underwent photolithography to

pattern a ridge waveguide on the p-side of the substrate. This was done using standard UV photolithography utilizing a contact mask and 5214EIR positive photoresist, which is then inverted. The mask itself consisted of several patterns to set the footprint for multiple devices with varying dimensions. This would allow for future experiments with devices of similar characteristics, but varying lengths. After patterning, the ridge was etched in an inductively coupled plasma (ICP) machine using BCl_3 as the etchant. To reduce the spreading of the injected current and improve the optical field confinement, the ridge was etched to just 0.1- μm above the active region of the device. Then liquid Benzocyclobutene (BCB) was spun onto the wafer and it was baked at 250°C. Once cured, the wafer was placed in a reactive ion etch (RIE) machine employing Oxygen and CHF_3 to remove the BCB until the surface of the ridge was clearly visible. The purpose of the BCB is to act as an electrical isolation layer for the p-metal in the spaces it still occupies.

Next the wafer undergoes another photolithography step to create the pattern for the metal contact. Using electron beam evaporation, a p-metal consisting of 500-Å titanium (Ti), 500-Å platinum (Pt), and 3000-Å gold (Au) is evaporated on to the wafer. It then goes through another metallization step this time consisting of Ti/Au. This step allows for an increase of the p-metal thickness to at least 1- μm for good metal step coverage over the edge of the ridge where the BCB can sometimes be over etched. Also, this soft evaporated Au provides a site for easier wire bonding without risking damage to the device. A third photolithography step is performed to create the pattern needed for ion implantation. In preparation for ion implantation, a thick layer of photoresist is applied over the entire wafer with clearances at the 5- μm gaps between each 250- μm section. The

wafer is then processed using proton implantation to electrically isolate each 250- μm section. The ion implantation provides greater than 10-M Ω of electrical isolation. It is important to note that the sections are only electrically isolated not optically. Then the wafer is lapped and polished using fine-grained aluminum oxide pads to produce a final thickness between 100- μm and 200- μm . This ensures high quality cleaved facets and sufficient thermal heat sinking. The backside of the wafer is then placed into the metal evaporator and the n-type metal consisting of Ge/Au/Ni/Au is evaporated on to the backside. The wafer is then annealed at 380°C. A higher temperature is not used because this would result in the cracking of the BCB and thus no longer providing the electrical isolation layer as desired. The ridge waveguide devices on the wafer are then cleaved in to several independent devices for testing. A simple depiction of this process is shown in Figure 2-6.

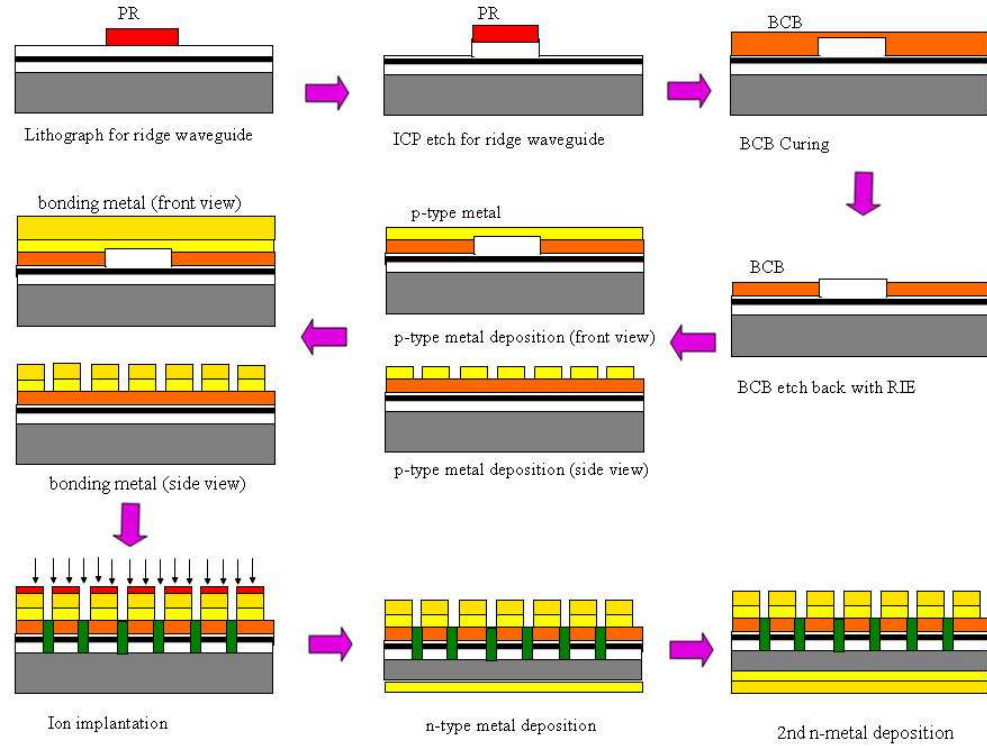


Figure 2-6 Standard processing for standard segmented contact devices [32]

A device 6.75 mm long, consisting of 27 250- μm sections, was cleaved off of the wafer to be used as the laser diode. The device's back facet, the cleaved facet near the absorber, received an HRC with a reflectivity of approximately 95% and the other facet received an ARC with reflectivity of approximately 5% to create a Fabry-Perot cavity. This single device is now ready to be mounted and tested. Figure 2-7 shows a diagram of the segmented device to be tested.

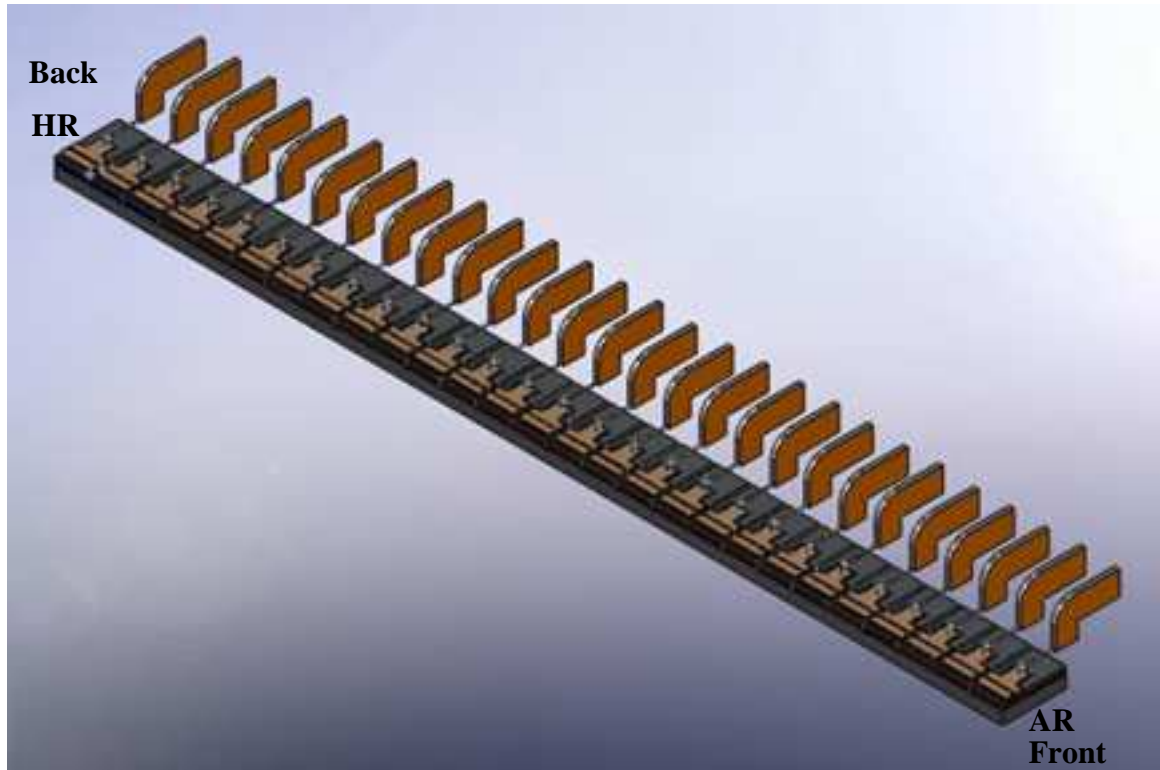


Figure 2-7 Segmented device

An Aluminum Nitride (AlN) substrate was mounted to a gold plated copper H-mount in order to provide a mounting location for the laser diode. The laser diode was then mounted onto the indium strip on the AlN, n-side down, for better heat sinking. The device is positioned so that the exit facet hangs over the edge of the AlN by less than 50- μm , this is to prevent any reflections and maximize heat sinking. Figure 2-8 shows the AlN substrates with 250- μm and the 500- μm contact pads that were used for mounting. Each of the laser diode's anodes was wire bonded to a 250- μm gold strip on the AlN as seen in Figure 2-9. The 250- μm gold strips were then hopped over to 500- μm gold strips on another AlN substrate permitting the device to be probed for testing.

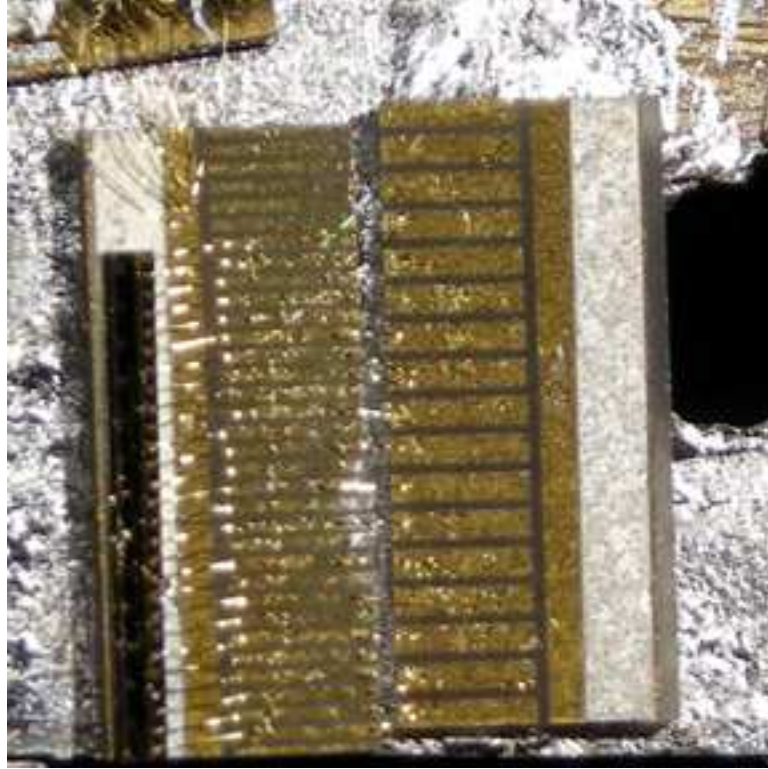


Figure 2-8 The 250- μm and 500- μm contact-pad AlN substrates

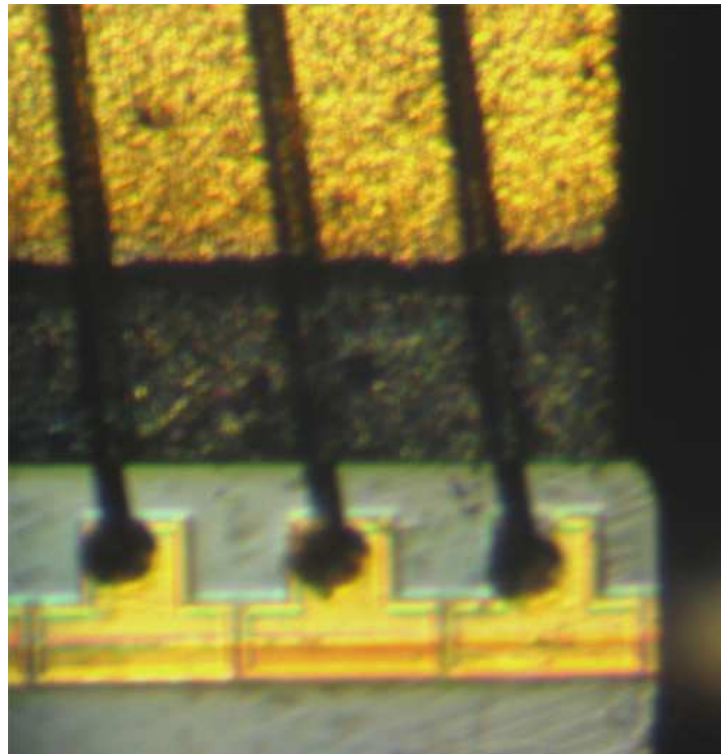


Figure 2-9 Wirebonding of the 250- μm anodes

2.4 Measurement Setup

After mounting the laser to the H-mount, it is ready to be placed on the stage. The stage consists of two copper blocks and a thermoelectric cooler (TEC). The H-mount is placed on a mounted piece of copper that is attached to the cold side of a TEC. The hot side of the TEC is attached to a bigger piece of copper allowing it to work as a heat sink by moving heat away from the device as seen in Figure 2-10. This allows for the device to be steadily cooled to 20 °C for the duration of the measurements.

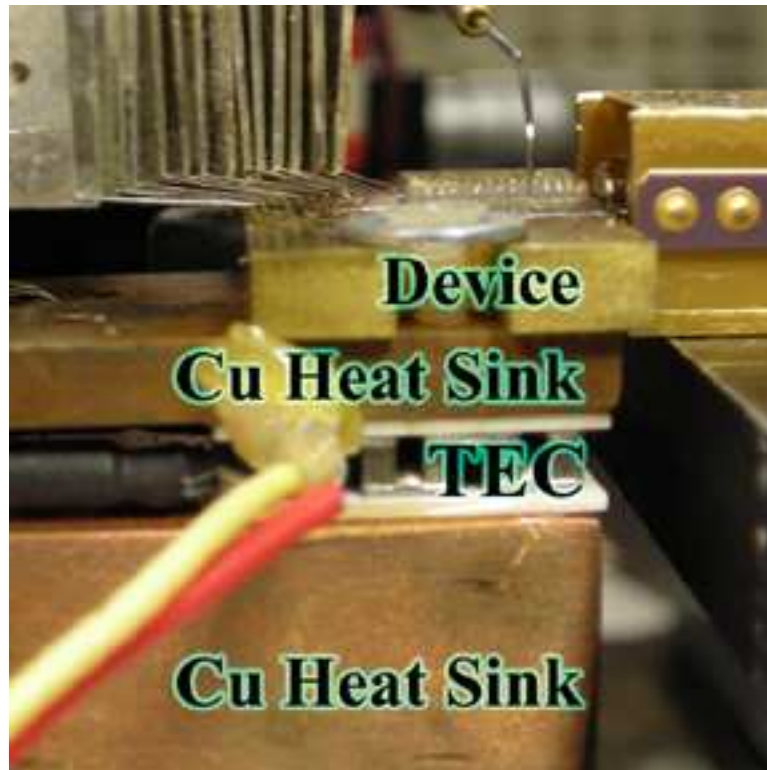


Figure 2-10 Side view of the copper stage with the TEC

Once the device is securely fastened to the copper stage, the probe card is moved into position. The probe card consists of 16 probes, each electrically isolated with a diameter of 0.75-mm, which are arranged to match the spacing of the 500- μm gold strips

on the AIN. The probe cards allows for the control of injection current and reverse bias voltage going into the device as seen in Figure 2-11. This allows for the ease of reconfigurability for running the tests. Also, the probes are kept away from the device to prevent any accidental scratching of the device.

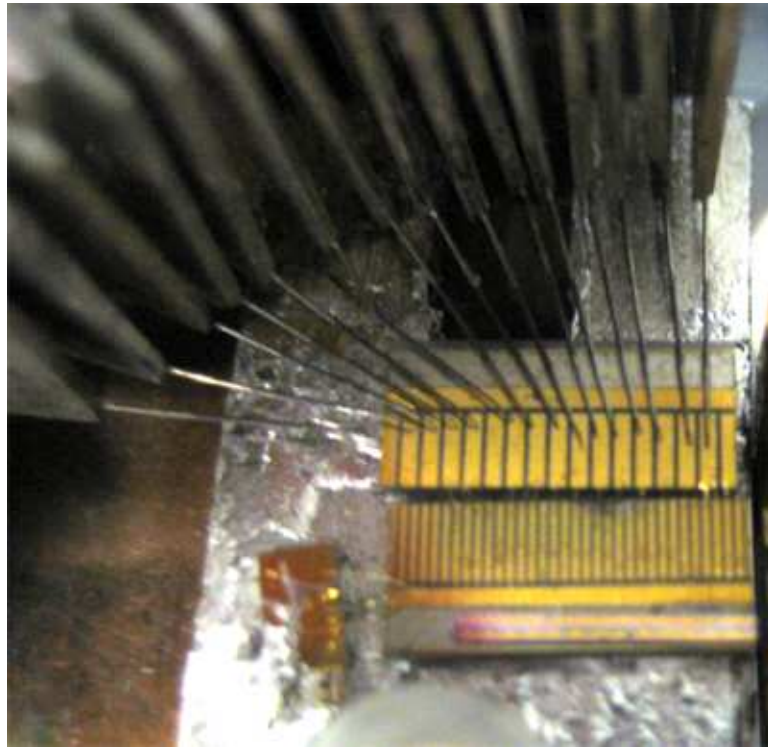


Figure 2-11 Probe card connected to device

The current is pumped into the device by a current source controlled by computer code in Igor Pro. The software controls the output of the ILX Lightwave LDC3916 Laser Diode Controller to correspond to the desired injection current. This allows for complete control of the current applied to each gain section and thus controls the operational conditions. The reverse bias, when desired, is applied by connecting an Agilent 3610A DC Power Supply to the necessary probe. As shown in Figure 2-12 any probe can be used to either apply a reverse bias or inject current.

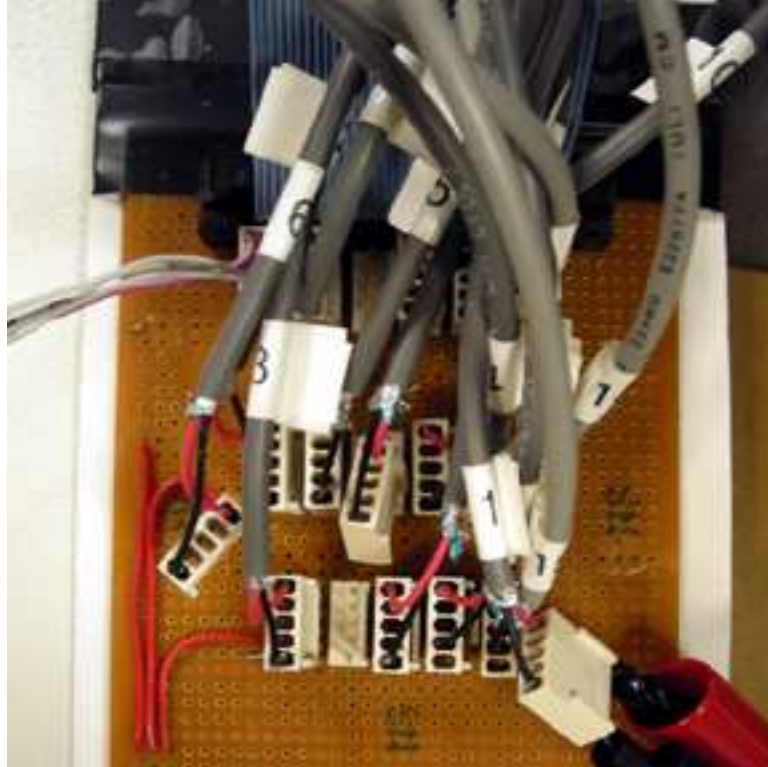


Figure 2-12 Reconfigurable board for biasing the laser

The light exiting the device was coupled into an optical head pigtailed with single mode polarization maintaining fiber. The optical head, 414F-GH-10, had a coupling efficiency of approximately 15% and was able to couple 0 to 1 dBm of the laser's light. The optical head was aligned to the laser's exiting facet using a five-axis stage. This stage allowed for more sensitive tuning, thus allowing the greatest amount of light to be coupled. Minor realignment was needed approximately every 15 to 30 minutes due to gravity pushing down on the stage's Z-direction translation. The alignment was made and monitored using an ILX Lightwave FPM-8210H Fiber Optic Power Meter to see the power of the coupled light. The optical head was aligned to the device until the maximum power was coupled, approximately 1 dBm. While running the experiment if the power exiting the optical head's pigtail dropped to 0 dBm, realignment was necessary.

In order to study the repletion rate of the device, an Electrical Spectrum Analyzer (ESA) and a photodetector were used. The light from the fiber pigtail of the optical head was coupled to a New Focus 45 GHz IR Photodetector Module 1014, which was connected to an Agilent 8565EC 50 GHz Spectrum Analyzer. This allowed for the measurement of the laser's repetition rate and quality of mode locking.

To ascertain the mode-locking behavior of the device, the pulse shape was also measured using an autocorrelator and oscilloscope. The optical head's pigtail was connected to a Femtochrome FR-103XL autocorrelator which was connected to a Tektronix TDS540 Digitizing Oscilloscope. This allowed for the viewing of the pulse shape and the emergence of pulses due to higher order harmonics. The measured pulse widths were then calculated using a Gaussian curve fit. Figure 2-13 is a schematic of the complete system with all of the associated components.

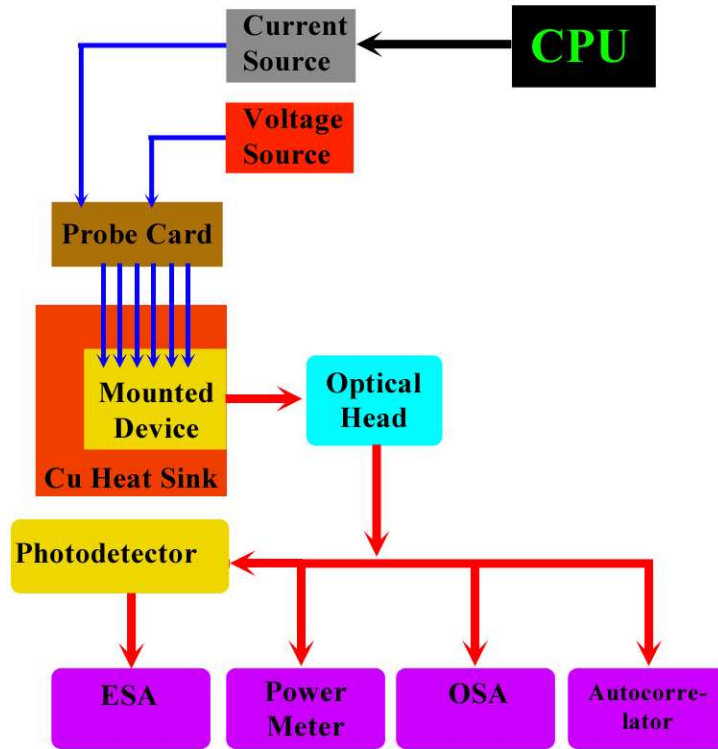


Figure 2-13 Complete system schematic

CHAPTER 3 - DATA AND MEASUREMENTS

3.1 Rationalization and Focus of the Experiment

With passive mode-locking there is a tradeoff between the compression of the pulse width and the quality of the mode-locking. The saturable absorber introduces a nonlinear element to the laser that allows for pulse widths to be trimmed/narrowed, but at the same time if the absorber section is too long then it limits the operational range of the device. As stated in Chapter 1, the goal of this thesis is to see if it is possible to stimulate higher order harmonics of the mode-locked laser utilizing the double interval technique exploited by violinists. This thesis will apply the double interval technique to a semiconductor laser by using the device's geometry and multiple absorber sections in order to stimulate higher order harmonics. Device symmetry is very important to the application of the double interval technique because of the locations of the saturable absorber sections directly correspond to the creation of anti-nodes as discussed in Chapter 2. The experiment will be successful if the sixth and/or tenth harmonics are excited using the double interval technique.

3.1.1 Fundamental Harmonic Laser Characteristics

The device used for the double interval higher order harmonic generation is a 6.75-mm long GaAs semiconductor laser diode, consisting of 27 250- μm sections. In order to have a starting point for this experimental effort, the laser's fundamental harmonic must be found. For the self-colliding pulse passively mode-locked system, the fundamental harmonic is found by placing the saturable absorber next to the HRC facet

[33]. With this device in particular, it was seen that with more than three continuous absorber sections ($>750\text{-}\mu\text{m}$) it was not possible to achieve mode-locking. This is valuable information because for the fundamental harmonics, the absorber length is limited by the mode-locking threshold conditions. Since the laser was not able to mode-lock while having four sections of continuous absorbers (1.00-mm) located at the HRC facet it would be impossible to maintain mode-locking while having 1.00-mm of absorber anywhere else in the device. The fundamental harmonic was observed when the device was configured with three continuous absorber sections ($750\text{-}\mu\text{m}$) located next to the HRC. Three sections were used because this would introduce the greatest amount of pulse trimming. The addition of more sections would shutdown the mode-locking of the device. As shown in Figure 3-1, the fundamental harmonic is accomplished by placing a reverse bias of 3.15 Volts across the last three sections (25, 26, and 27), as indicated by the blue probes. The remaining sections (1-24) are pumped with 150 mA distributed equally across the gain section length (555.56 A/cm^2), as shown by the red probes. The values for the reverse bias and pumping current were selected experimentally in order to maintain the minimum of 0 dBm output power needed to take the measurements. Figure 3-2 shows the fundamental and higher harmonics of the laser across a 50 GHz span and Figure 3-3 shows a 100 MHz span of the fundamental frequency. It is explicit from Figure 3-3 that the fundamental frequency for this laser is 6.019 GHz. Figure 3-3 is useful for seeing the quality of the mode-locking because it shows the peak intensity with respect to the noise floor. For this thesis the device will be considered mode-locked as long as there is at least 15 dB of signal between the noise floor and the peak of the ESA measurement. Figure 3-4 shows the pulse width associated with the fundamental

harmonic having a Full Width at Half Maximum (FWHM) of 4.96 ps. The higher order harmonics of the laser will be integer multiples of the fundamental frequency. For example, for a 6.0 GHz fundamental frequency the frequencies corresponding to the second, third, fifth, and tenth harmonics would be 12.0 GHz, 18.0 GHz, 30.0 GHz, and 60.0 GHz, respectively.

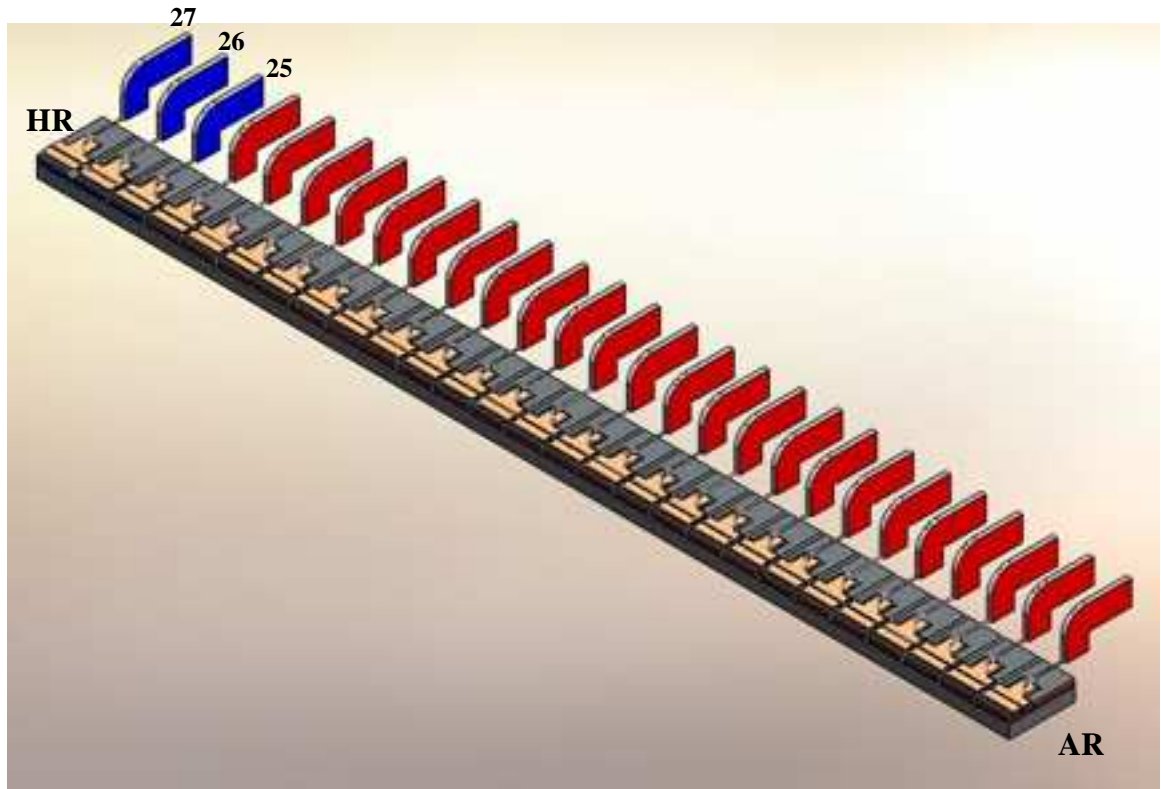


Figure 3-1 Configuration for the generation of the fundamental harmonic

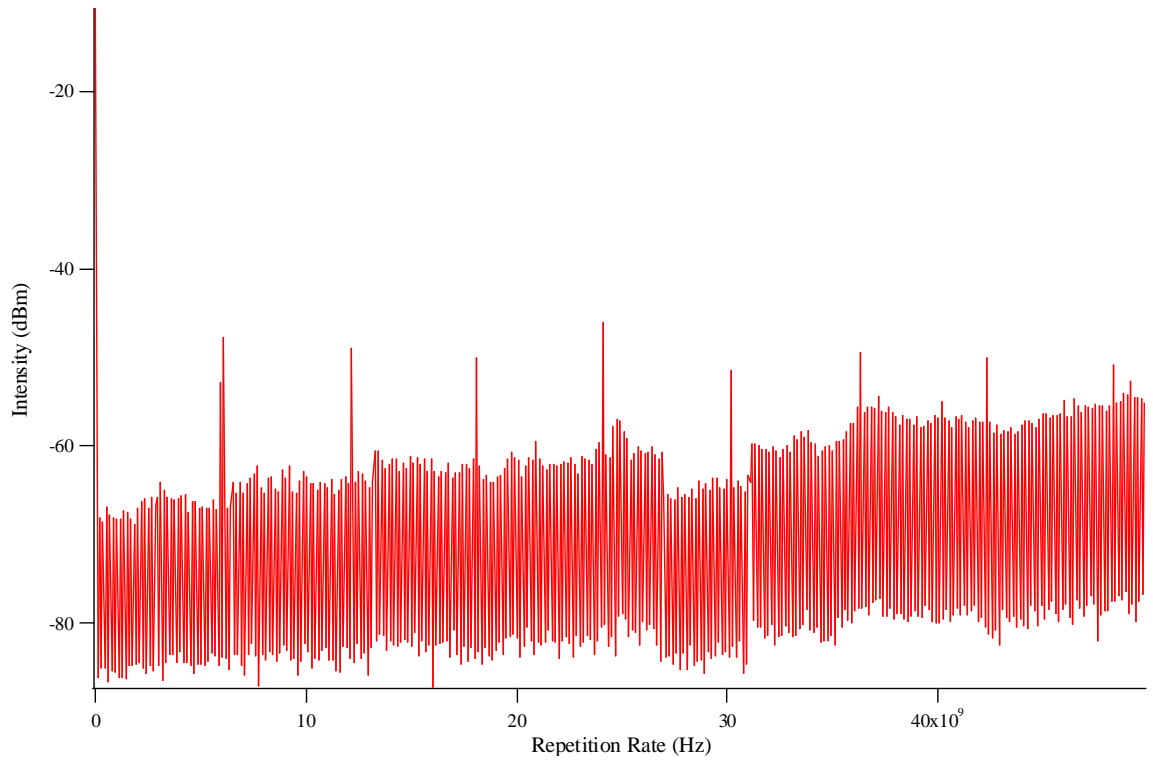


Figure 3-2 50 GHz span of the laser diode's fundamental repetition rate

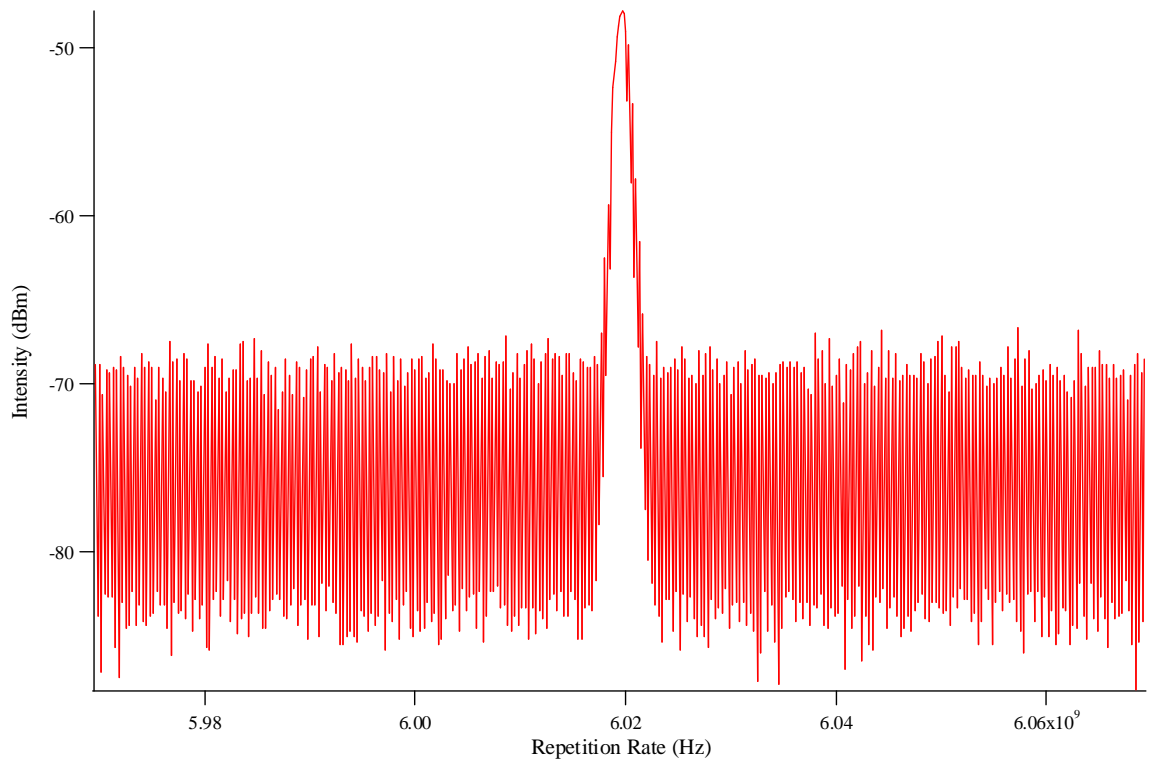


Figure 3-3 100 MHz span of the fundamental repetition rate

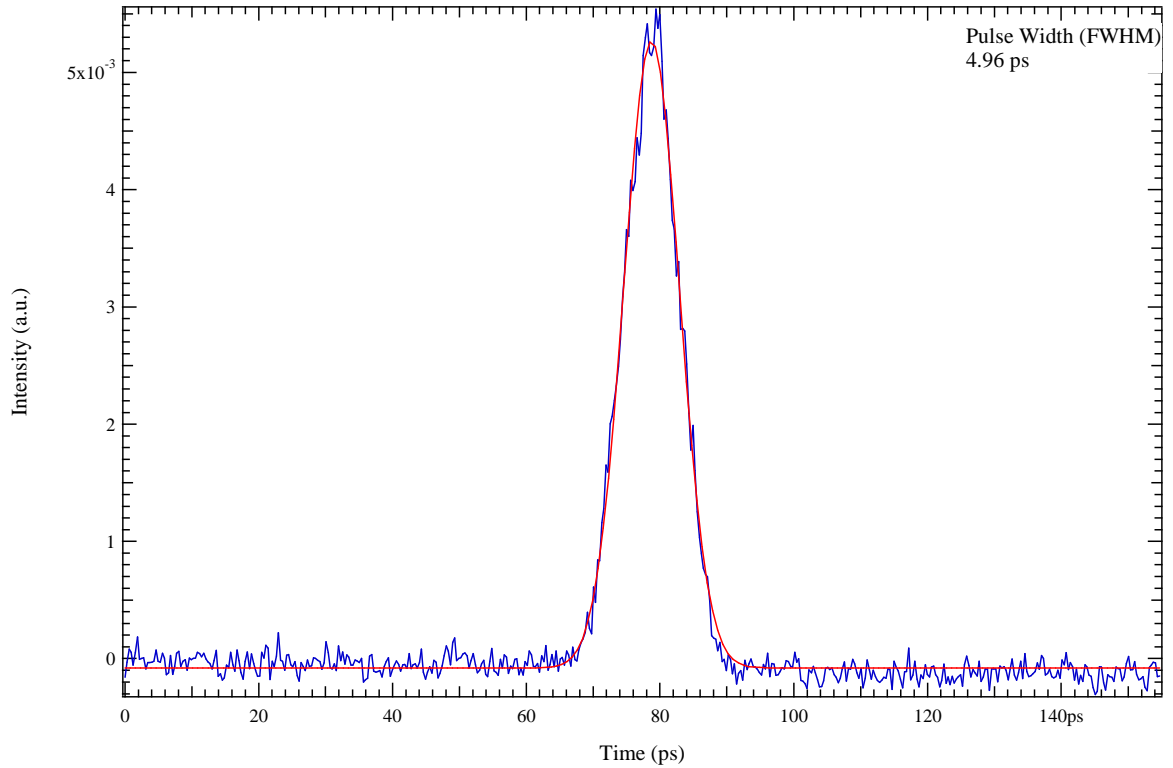


Figure 3-4 Pulse width associated with the fundamental harmonic repetition rate

3.1.2 Second Harmonic Laser Characteristics

To generate the laser's second harmonic, the saturable absorber is placed in the center of the laser's gain cavity. As stated earlier, symmetry is very important when stimulating higher order harmonics. Section 14 is the midpoint of the 27 section device. It is desired to have the point of symmetry as close to the middle of the saturable absorber as possible. By ensuring that the midpoint of the saturable absorber is at the desired division of the cavity length, it is easier to stimulate the desired harmonic. To excite the second harmonic there are two main options, using one saturable absorber (section 14) or using three saturable absorbers (sections 13-15). With both methods symmetry will remain, but due to the fact that the end goal of this thesis is to apply the second harmonic

towards the double interval technique, the second harmonic is stimulated using just one absorber. The advantage of having sections 13-15, Figure 3-5, as saturable absorbers is that with the longer absorber length the pulse is trimmed more. This is apparent when comparing the pulse widths of Figure 3-6 which is for the three sections absorber case and Figure 3-10 which is the one section absorber case. This will guarantee that the additional saturable absorber sections can still be placed within the cavity without jeopardizing the mode-locking conditions.

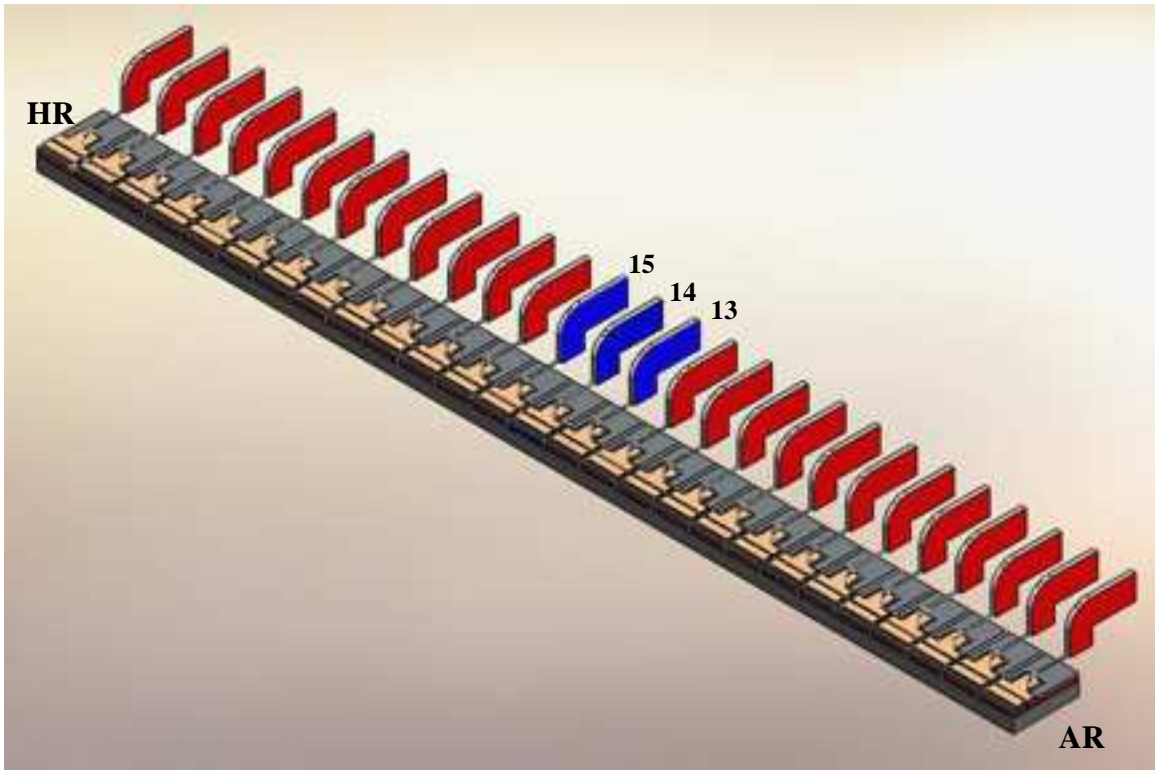


Figure 3-5 Configuration for the generation of the second harmonic using three saturable absorbers

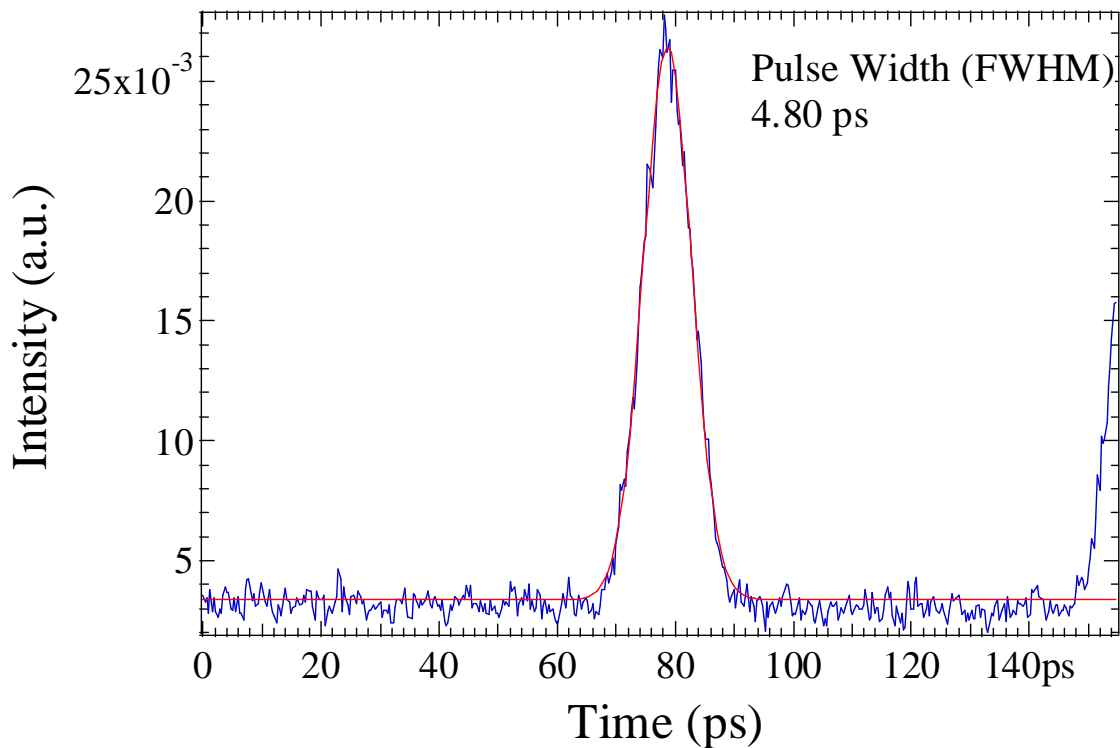


Figure 3-6 Pulse width associated with the second harmonic repetition rate for when three sections of saturable absorber is used

Optimal Second Harmonic Configuration and Laser Characteristics

The optimal configuration was when section 14, as shown in Figure 3-7, was chosen as the absorber section and it was biased at 4.49 Volts, as shown with the blue probe. The increase in voltage compared to the fundamental harmonic case is mainly due to the fact that the absorber section is limited to only 250- μm and that it must provide adequate absorption. The remainder of the laser diode was uniformly pumped with 150 mA (555.56 A/cm²), as shown with the red probes. Figure 3-8 shows the set of harmonics that generate the pulses at the second harmonic repetition rate of the laser across a 50 GHz span. Figure 3-9 shows a 100 MHz span of the second harmonic repetition frequency. As shown in the figures, the second harmonic frequency for this

laser is 12.027 GHz. Figure 3-10 shows that the pulse width associated with the second harmonic having a FWHM of 7.28 ps.

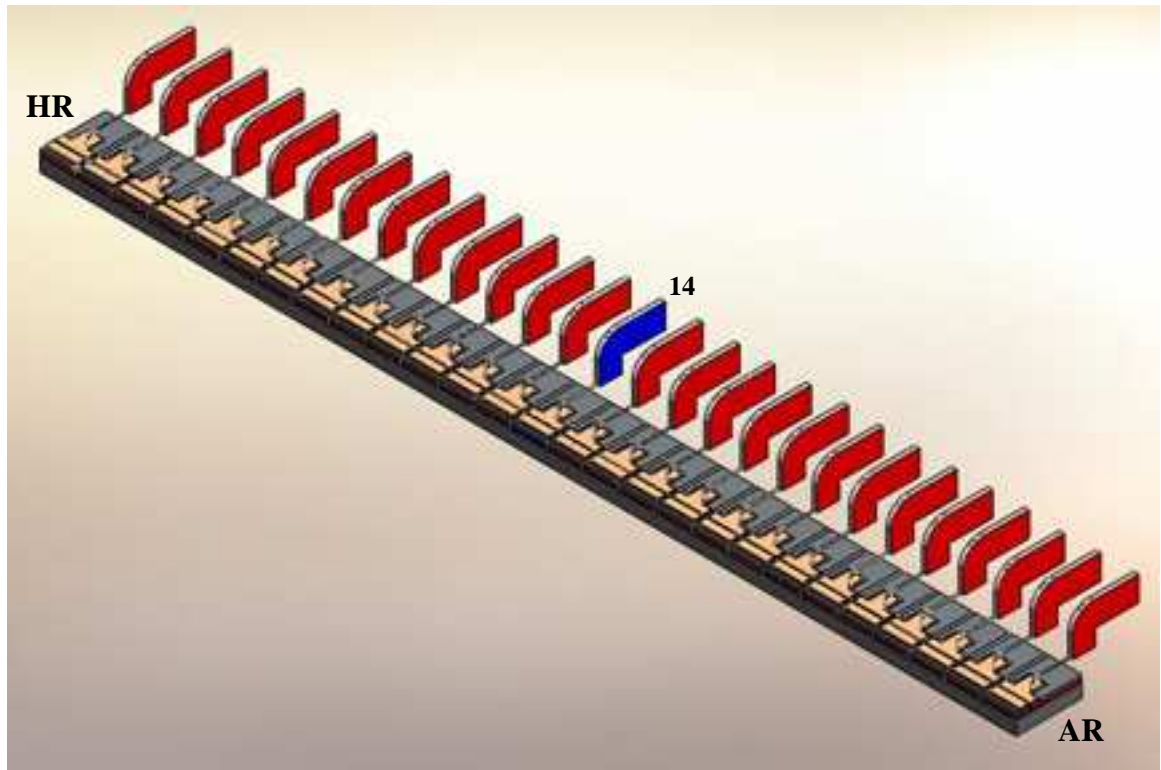


Figure 3-7 Configuration for the generation of the second harmonic

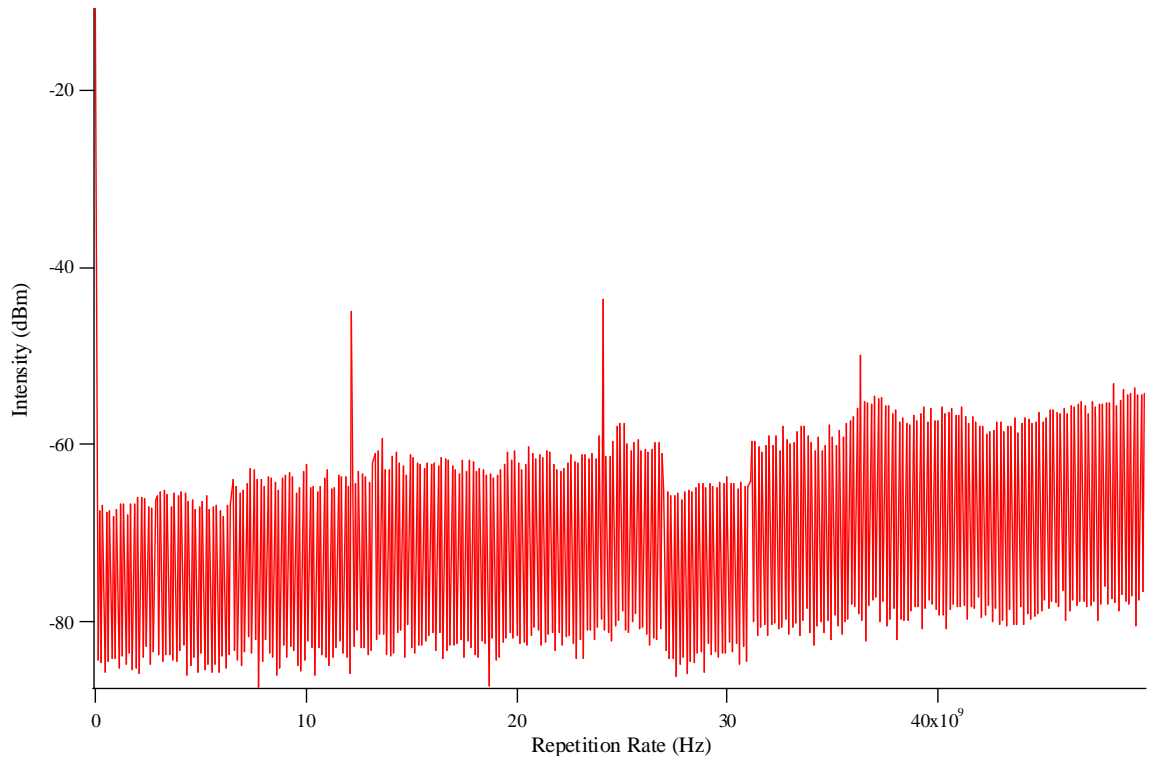


Figure 3-8 50 GHz span of repetition rate while configured for second harmonic generation

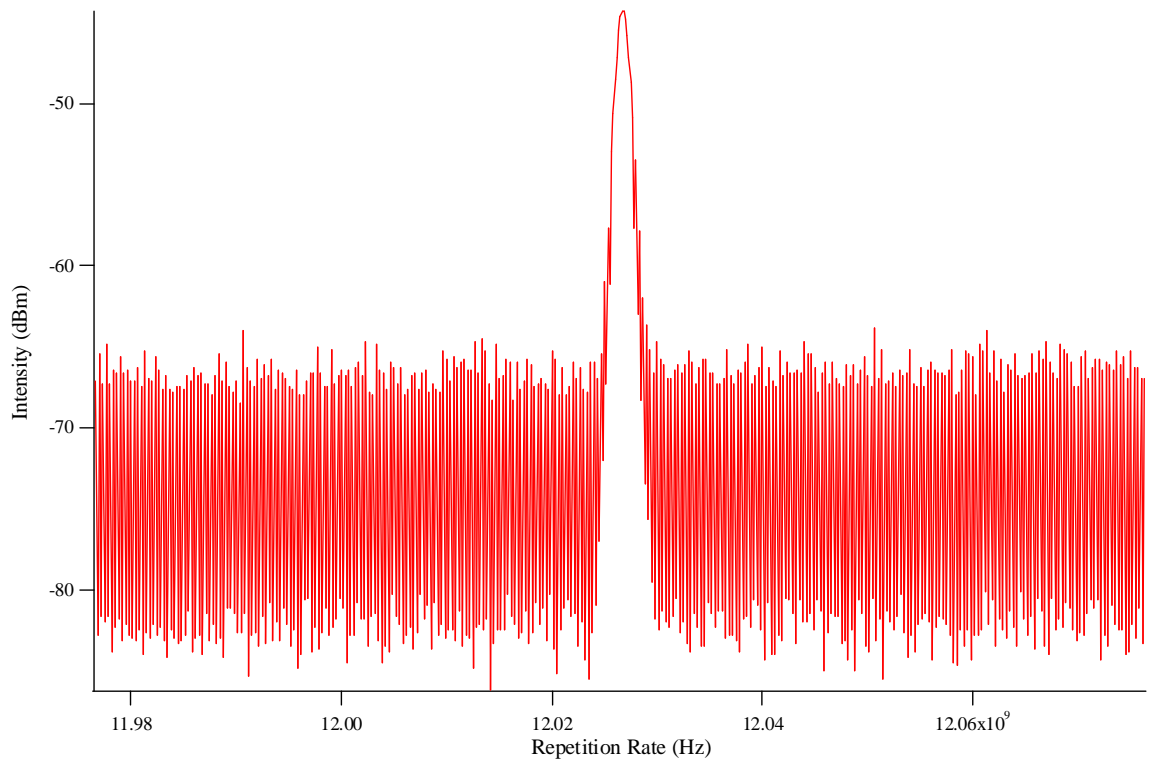


Figure 3-9 100 MHz span of the second harmonic repetition rate

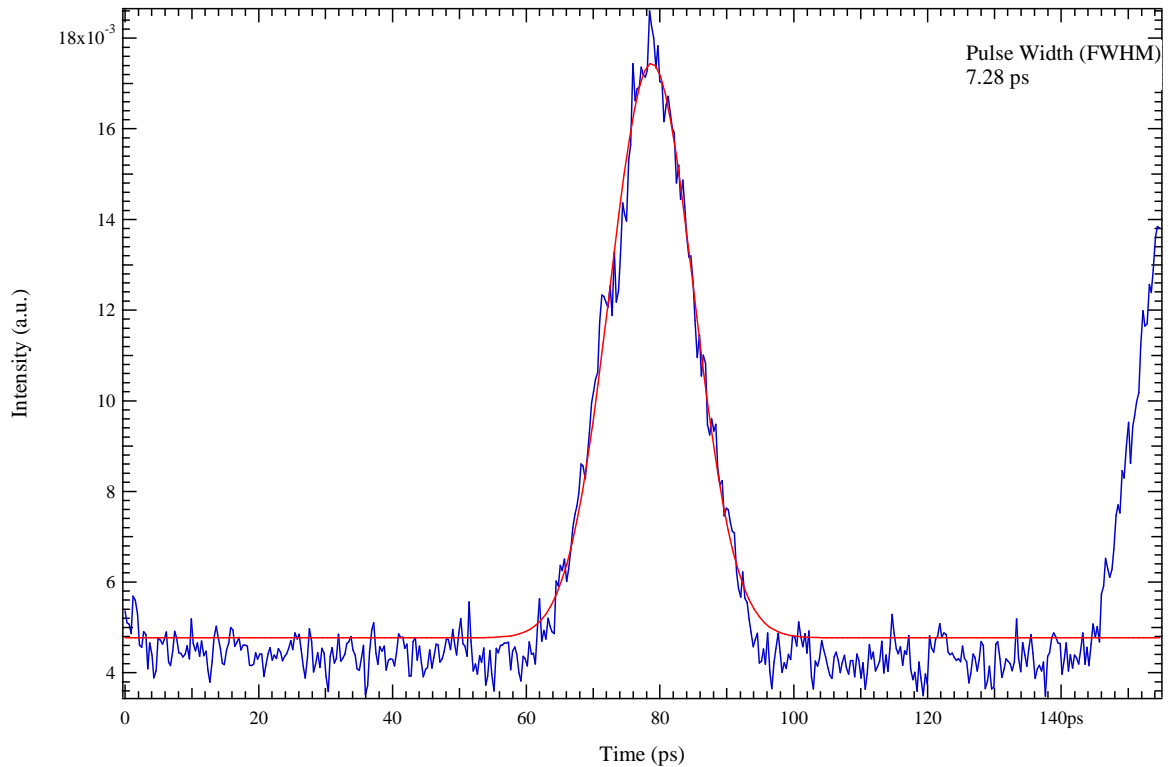


Figure 3-10 Pulse width associated with the second harmonic repetition rate

3.1.3 Third Harmonic Laser Characteristics

To generate the laser's third harmonic, the saturable absorber needs to be placed at a location approximately one third of the laser's total length from either facet. One third of the 27 section device would correspond to 9 sections from either facet. The issue is that the saturable absorber's center needs to be placed with its center located in a spot where the pulse has already traveled through 9 sections. This would correspond to the area in between the two adjacent sections. Since it is not possible to place a reverse bias at this location specifically, two saturable absorbers are used to create an absorption section that would have a midpoint corresponding to the desired symmetry. Placing saturable absorbers one third from either facet would correspond to placing a reverse bias

at sections 10 and 9 or 18 and 19 or both as seen in Figure 3-11. In Figure 3-11(a), the saturable absorber section is too close to the emitting facet and this causes difficulty in having the device mode-lock. In Figure 3-11(b), we achieve the optimal condition and this will be discussed in the following sections. For Figure 3-11(c), mode-locking is shutdown and the laser operates in continuous wave (c.w.) because as stated earlier, once four sections are used as the saturable absorber, mode-locking is lost. Thus the configuration in Figure 3-11(c) is ruled out.

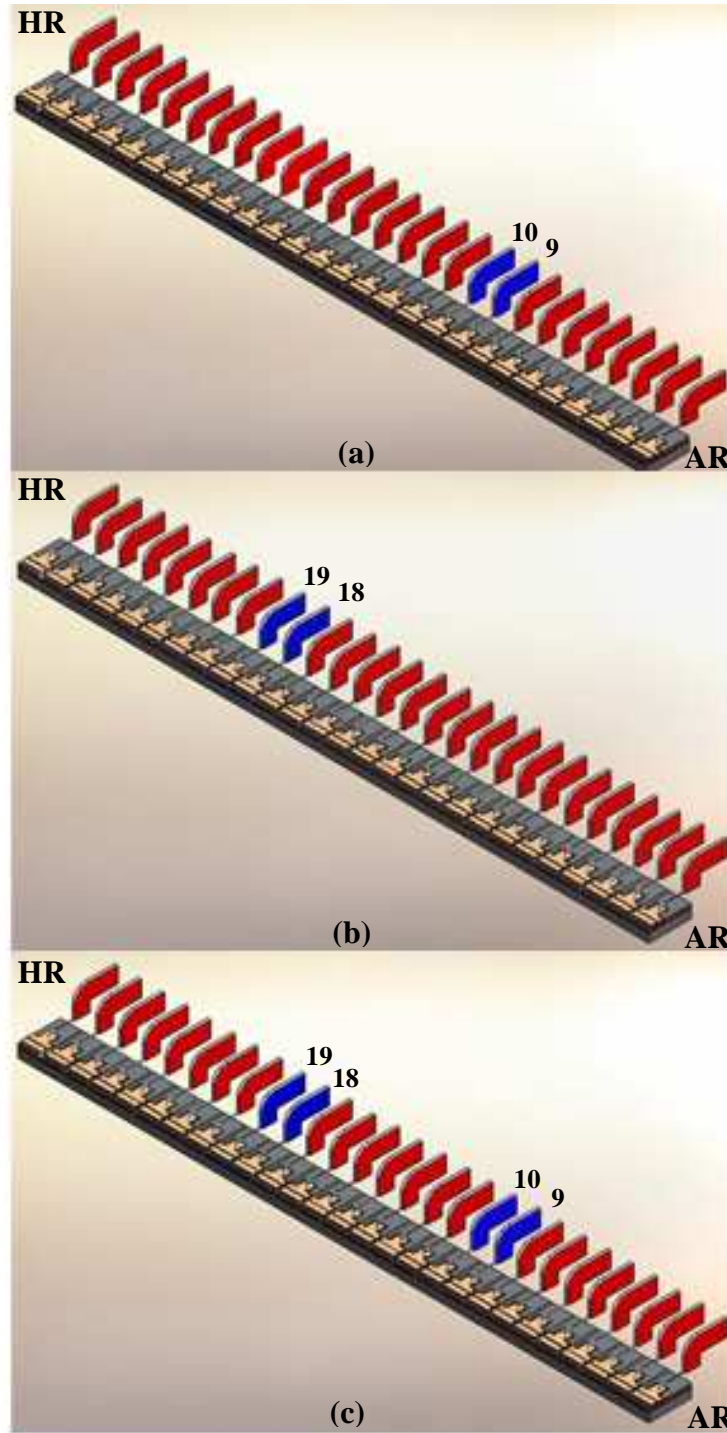


Figure 3-11 Possible configurations for the generation of the third harmonic. (a) Using only sections 9&10, (b) using only sections 18&19, and (c) using sections 9&10 and 19&18

Optimal Third Harmonic Configuration and Laser Characteristics

The optimal case for the third harmonic was achieved when sections 18 and 19 were used as the saturable absorber as seen in Figure 3-12. This is due to the saturable absorber's proximity to the HRC facet because it is easier for the device to mode-lock when the absorber section is closer to the HRC because of the high photon density and the possibility of higher modulation depth. The sections were reverse biased with a voltage of 3.38 Volts, as shown with the blue probes. The remainder of the laser diode was uniformly pumped with 150 mA (555.56 A/cm^2) to ensure the average power of 0 dBm needed in order to carry out the experiment, as shown with the red probes. Figure 3-13 shows the set of harmonics that generate pulses at the third harmonic repetition rate and Figure 3-14 shows a 100 MHz span of the third harmonic's repetition frequency. As can be seen in the figures, the third harmonic frequency for this laser is approximately 18.023 GHz. Figure 3-15 shows the pulse width associated with the third harmonic having a FWHM of 4.34 ps.

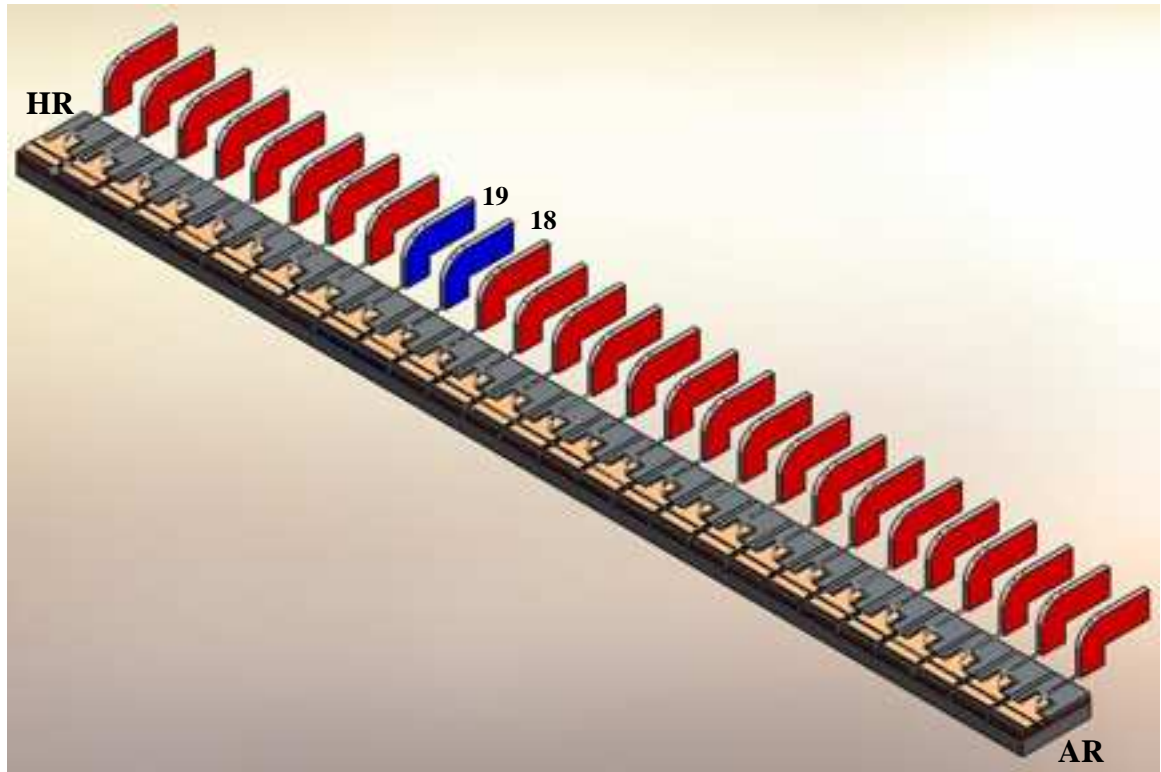


Figure 3-12 Configuration for the generation of the third harmonic

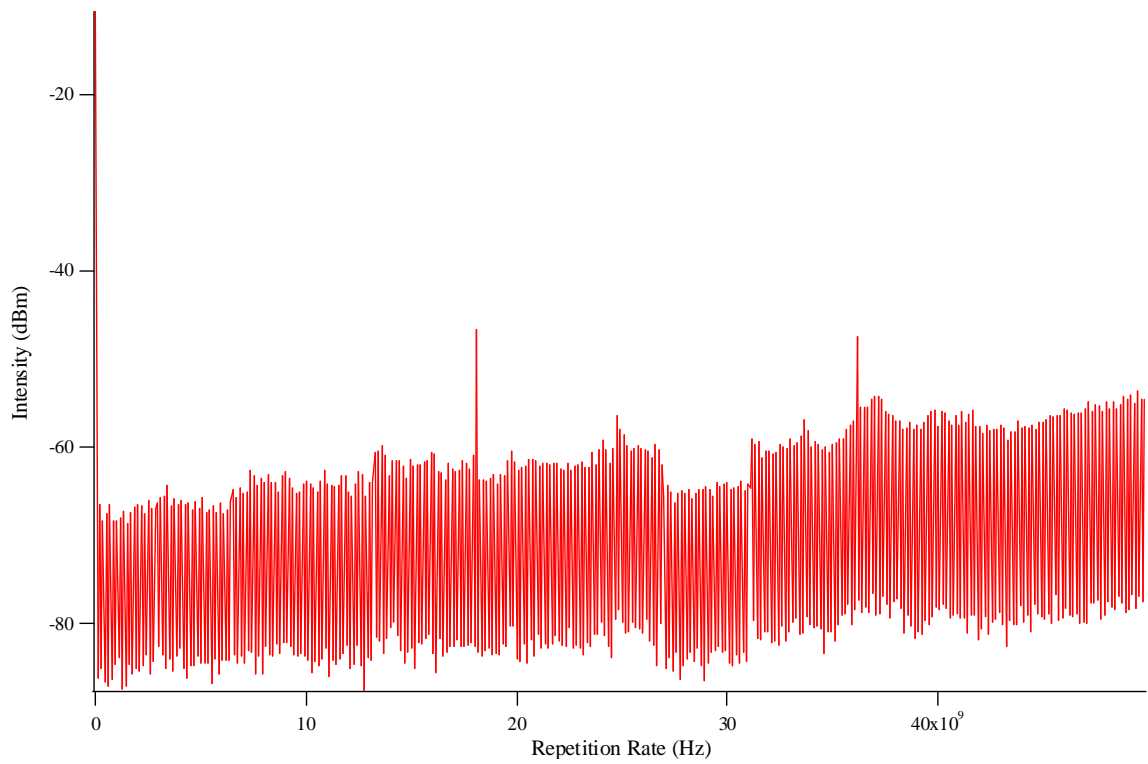


Figure 3-13 50 GHz span of repetition rate while configured for third harmonic generation

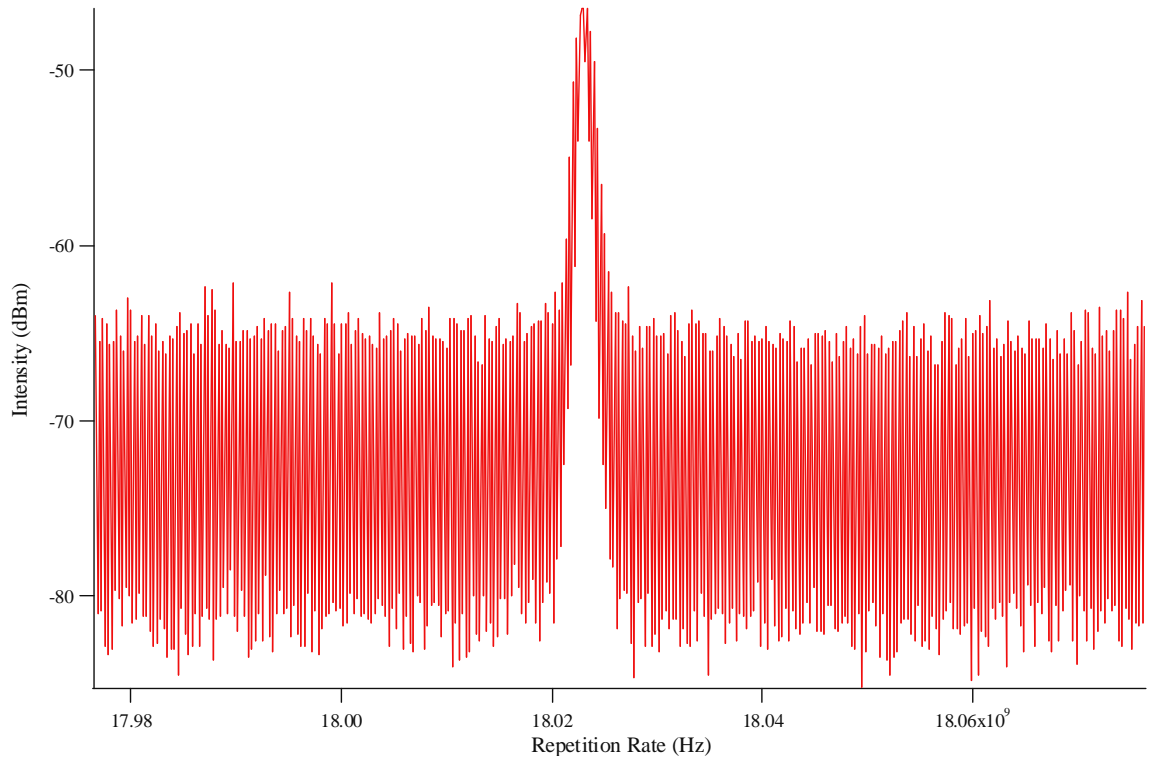


Figure 3-14 100 MHz span of the third harmonic repetition rate

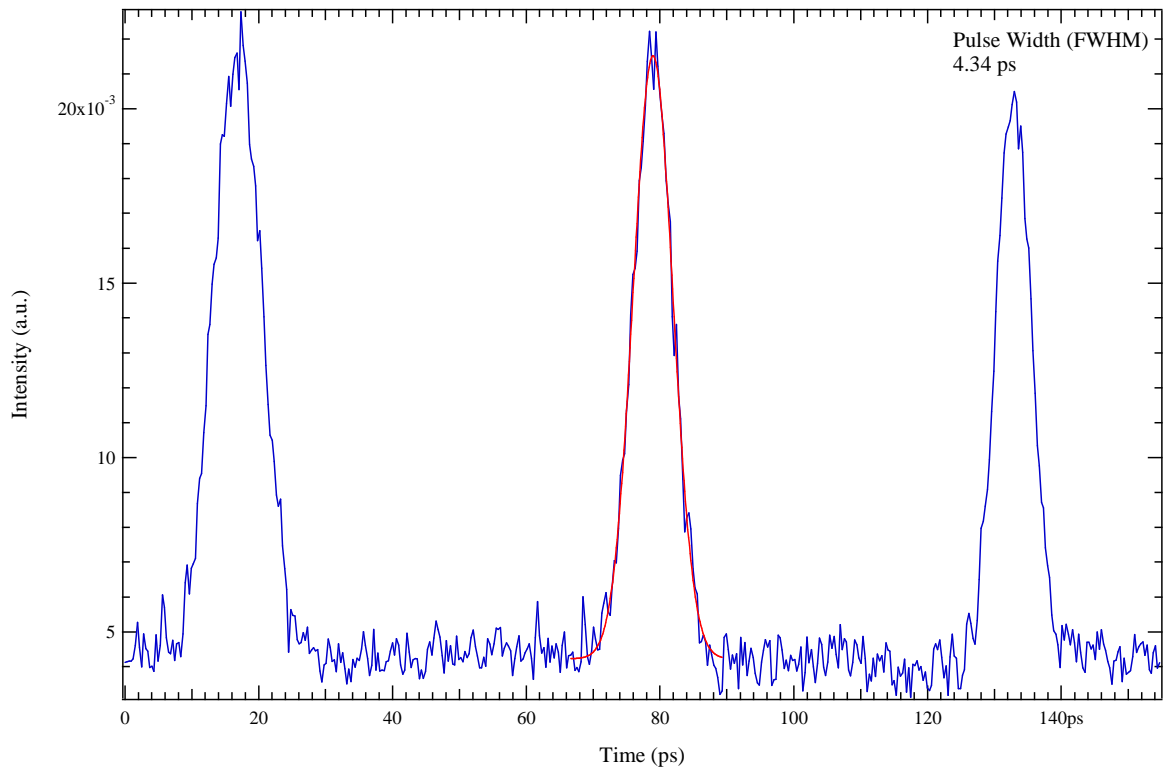


Figure 3-15 Pulse width associated with the third harmonic repetition rate

3.1.4 Fifth Harmonic Laser Characteristics

To generate the laser's fifth harmonic, the saturable absorber is placed at a location approximately one fifth of the laser's total length from either facet. One fifth of the 27-section device would correspond to 5.4 sections from either facet. By placing a saturable absorber at 6 sections from either facet it would be very close to achieving the 5.4 sections needed to stimulate the fifth harmonic since the center of the sixth section would be at 5.5. Again the minimum number of absorbers is used at each symmetric location because of the desired application toward the double interval technique later on in the experimentation. Placing a saturable absorber at a location one fifth from either facet corresponds to placing a reverse bias at section 6 or section 22 or both as seen in Figure 3-16. In Figure 3-16(a), the saturable absorber is too close to emitting facet to maintain stable mode locking, the colliding pulses are too asymmetric in power. In Figure 3-16(b), mode-locking was achieved, but the best condition was achieved with the configuration see in Figure 3-16(c). Stimulation of the fifth harmonic was successful for two cases - when the saturable absorber was placed at section 22 and when multiple saturable absorbers were used by placing one at sections 22 and 6 simultaneously.

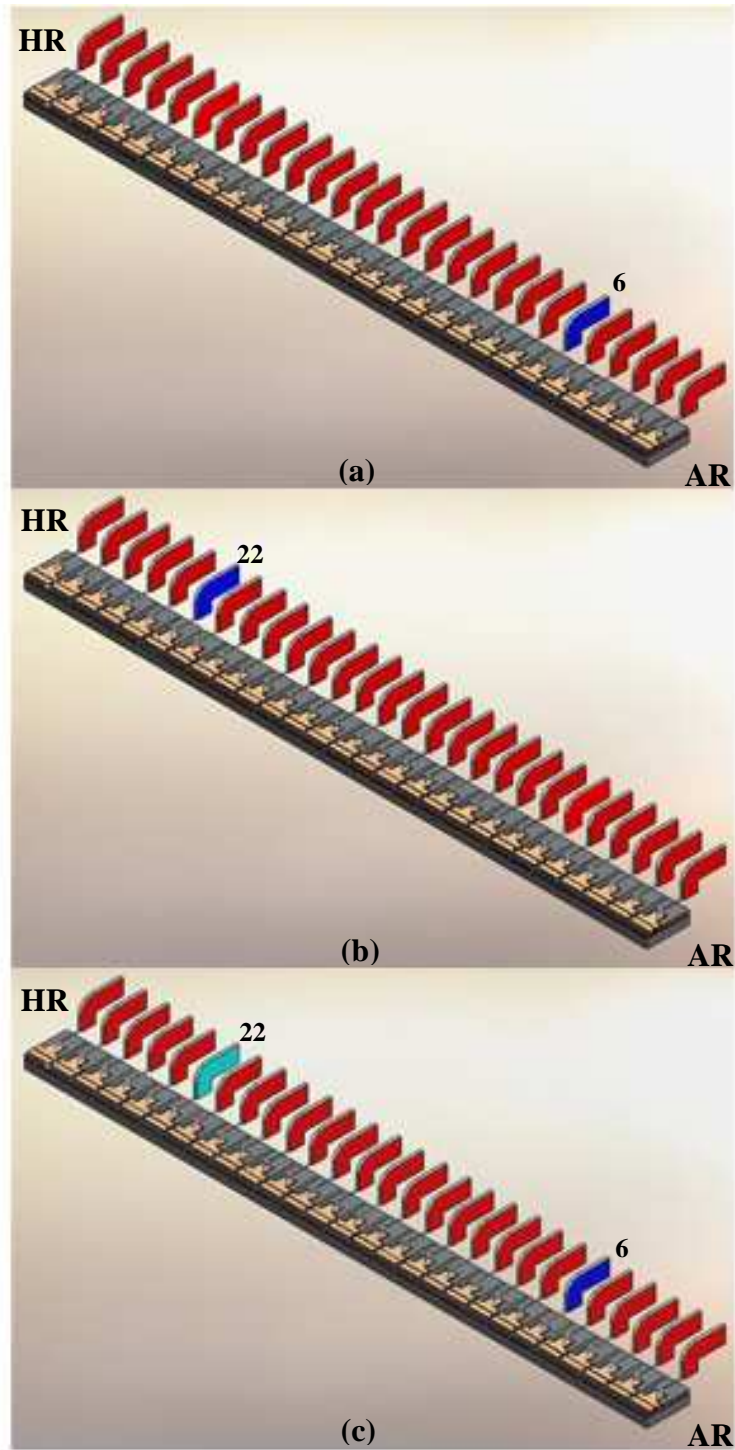


Figure 3-16 Possible configuration for the generation of the fifth harmonic. (a) Using only section 6, (b) using only section 22, and (c) using section 6 and 22

Optimal Fifth Harmonic Configuration and Laser Characteristics

The optimal case for stimulating the harmonic was achieved when both sections (22 and 6 simultaneously) were used as the saturable absorbers as seen in Figure 3-17. This also corresponded to the smallest pulse width for the fifth harmonic. This is due to the fact that by having two saturable absorber sections the pulse can undergo more trimming before it is coupled out of the system. It gives the pulse an opportunity to be trimmed at section 22 and again at section 6 prior to exiting the system. Section 22 was biased with a reverse voltage of 4.03 Volts, as indicated by the light blue probe, while section 6 received a reverse voltage of 2.10 Volts, as shown with the blue probe. Section 22 received a greater reverse bias because of its proximity to the high photon density created at the HRC facet end of the cavity. The remainder of the laser diode was uniformly pumped with 200 mA (740.74 A/cm^2), as shown with the red probes. The increase in pumping current is due to the fact that more of the laser is now under a reverse bias and more current is needed in order to mode-lock the laser. Figure 3-18 shows the fifth harmonic's repetition rate of the laser across a 50 GHz span and Figure 3-19 shows a 100 MHz span of the fifth harmonic's repetition frequency. As shown in the figures, the fifth harmonic frequency for this laser is approximately 30.125 GHz. Figure 3-20 shows the pulse width associated with the fifth harmonic having a FWHM of 4.96 ps.

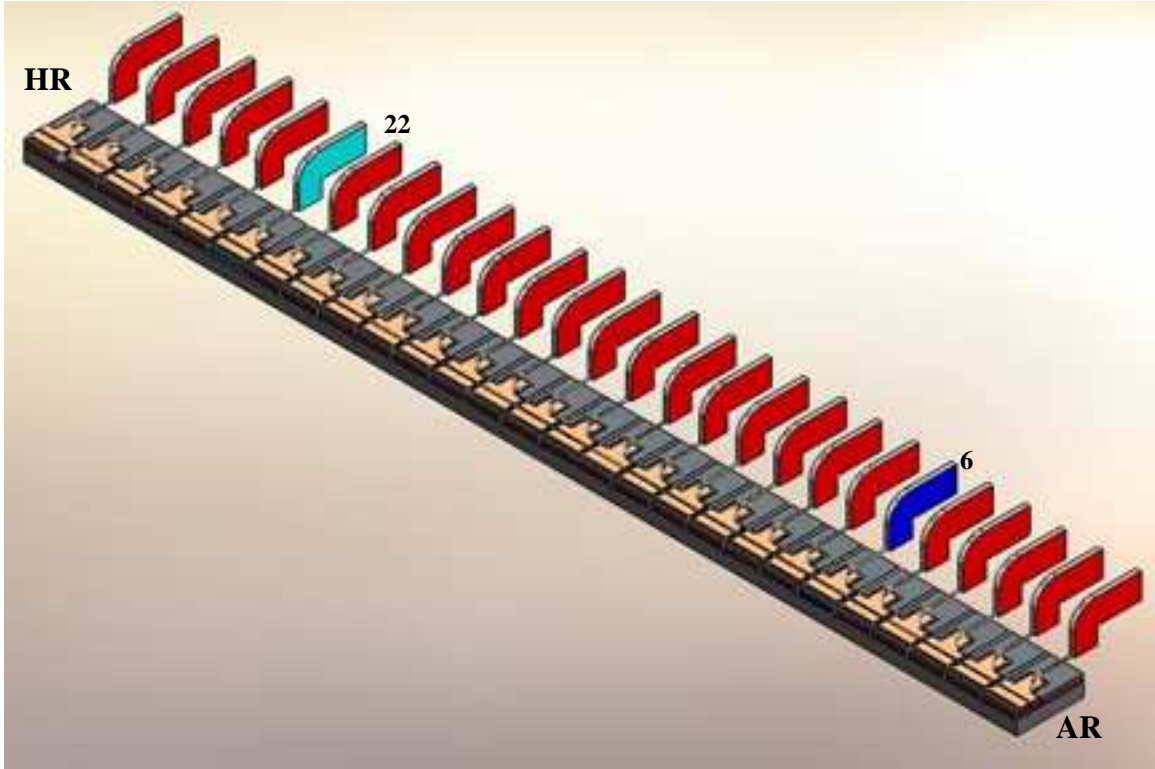


Figure 3-17 Configuration for the generation of the fifth harmonic

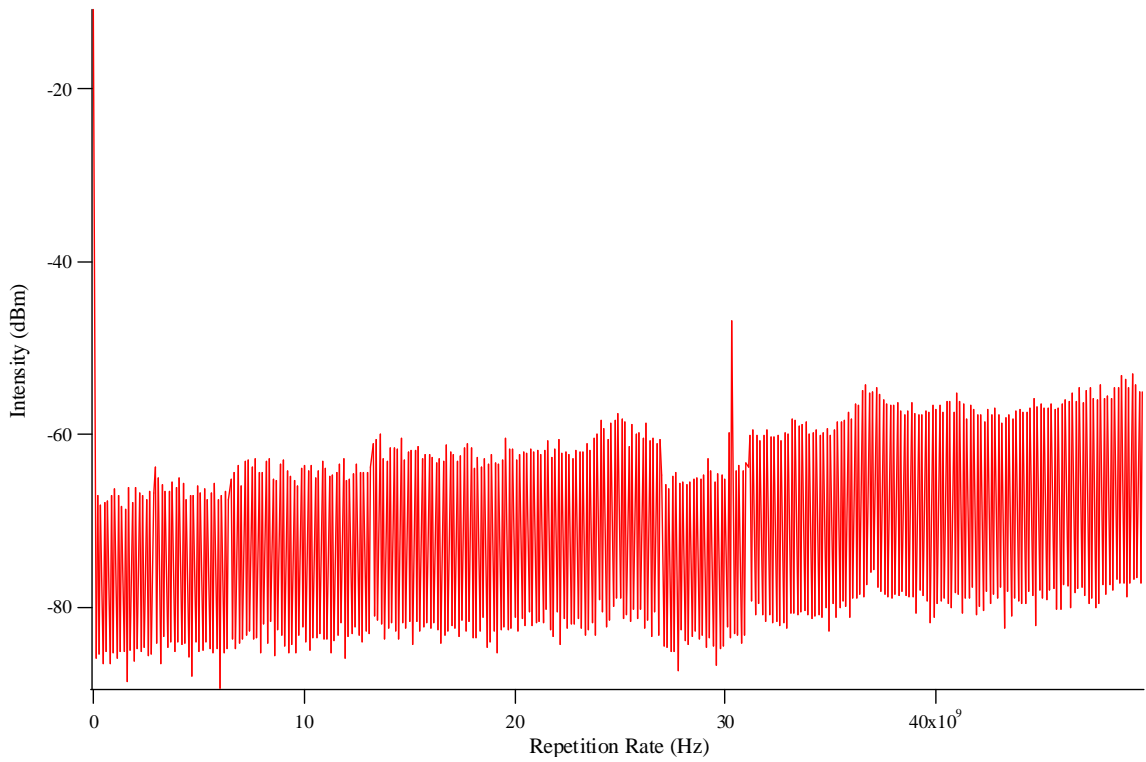


Figure 3-18 50 GHz span of repetition rate while configured for fifth harmonic generation

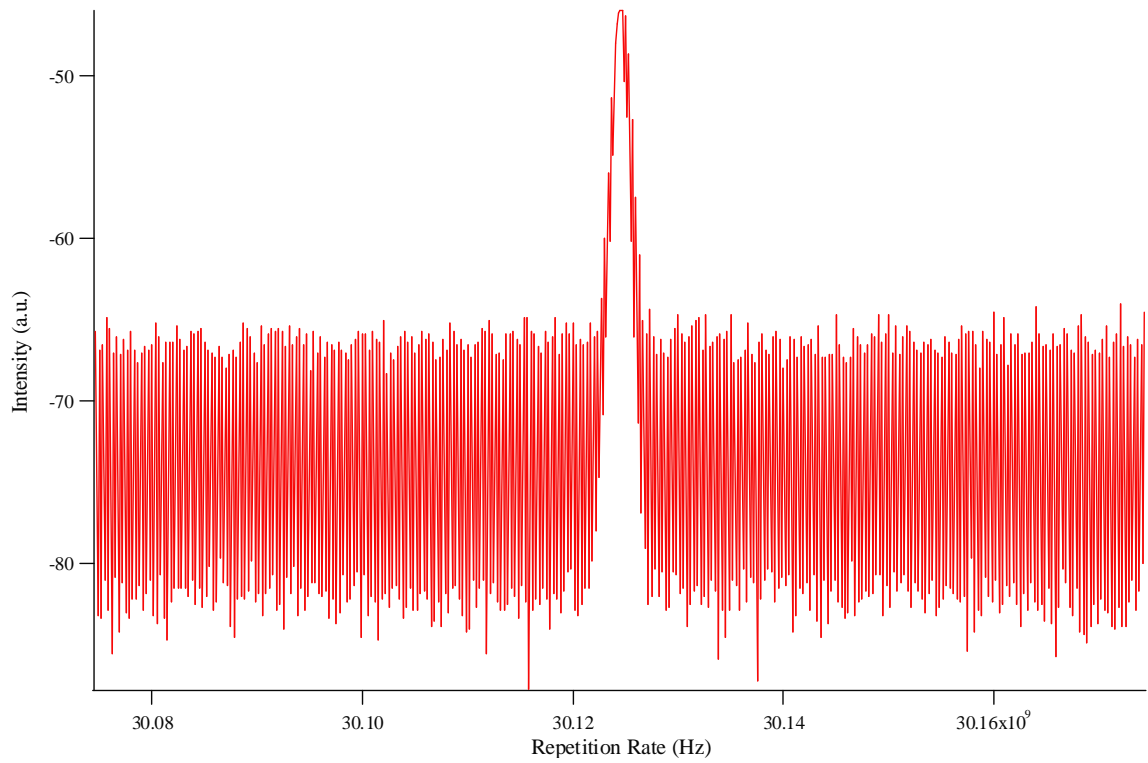


Figure 3-19 100 MHz span of the fifth harmonic repetition rate

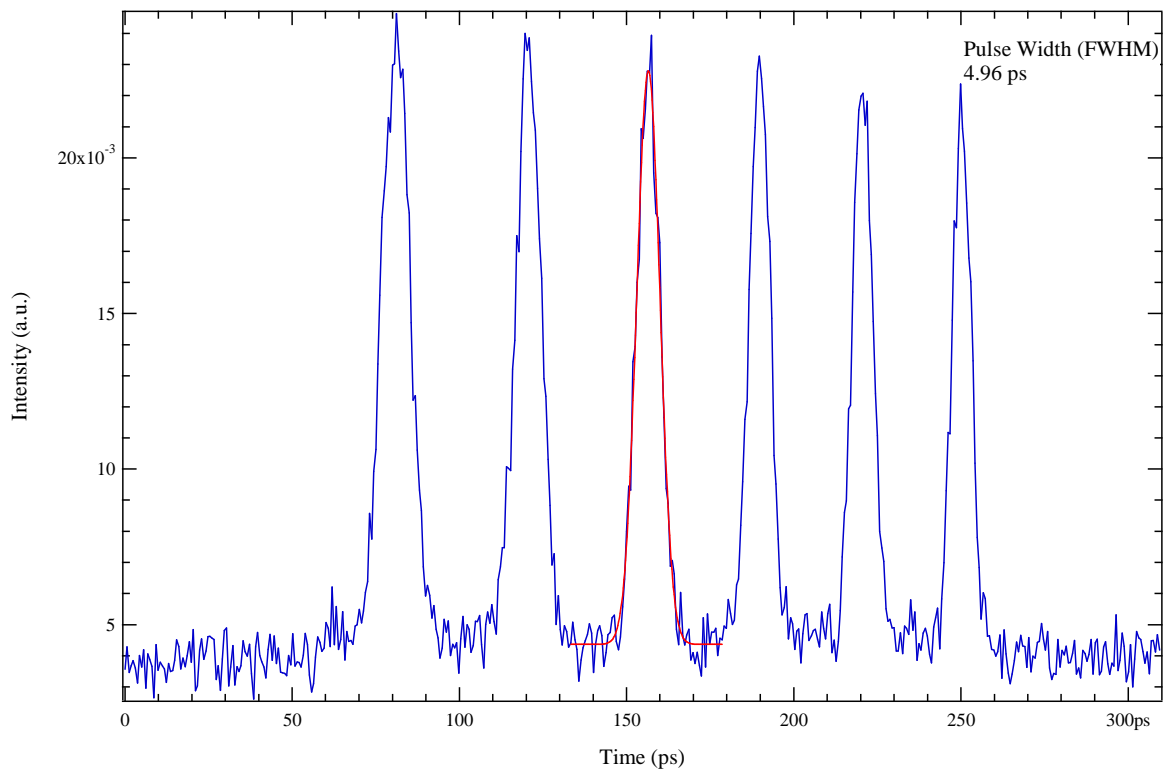


Figure 3-20 Pulse width associated with the fifth harmonic repetition rate

3.2 Double-Interval Experimentation

For the double-interval technique it is important that the saturable absorber sections work together in order to achieve higher harmonic stimulation. The double-interval technique results in harmonic mode-locking at the least common multiple of the individual absorber positions that correspond to certain lower harmonics. As shown in the 50 GHz ESA spans of each harmonics in Section 3.1, multiples of the harmonic are apparent when the prime is stimulated. For example Figure 3-8 shows the series of harmonics of the second harmonic repetition rate corresponding to 12.1 GHz, 24.2 GHz, and 36.3 GHz. The subsequent frequencies of the 12.1 GHz are just multiples of the lowest 12.1 GHz frequency. The double-interval technique generates the least common multiple of the harmonic frequency excited in the laser cavity. As discussed earlier placing a saturable absorber with the correct device symmetry is of immense importance. Once the 14th section is used for the stimulation of the second harmonic it is of no benefit to attempt to stimulate additional harmonics using sections 15-27. This is because the pulse loses the necessary intensity in section 14 so that it can collide with the opposing pulse with comparable intensity in the saturable absorber near to the ARC facet. Just as with the acoustic harmonics, the additional node/anti-node needs to be placed closer to the outputting facet so that the two nodes can work in unison to produce the higher order harmonic. The double-interval technique produces the least common multiple of the constituent absorber placements. The following experiments will show the combination of the second and third harmonics to stimulate the sixth harmonic and the use of the second and fifth harmonics to stimulate the tenth harmonic.

3.2.1 Sixth Harmonic Laser Characteristics

To generate the laser's sixth harmonic, the saturable absorber could be placed at a location approximately one sixth of the laser's total length from either facet as seen in Figure 3-21. Figure 3-21(a) and Figure 3-21(b) show the traditional method for stimulating the sixth harmonic. This could be impractical depending upon the laser's length. As lasers continue to become smaller and smaller it will become increasingly difficult to pattern sections small enough to create a region that can be easily biased and are unambiguously positioned to stimulate a certain harmonic. Since this thesis is geared to testing the double interval techniques, these configurations were not tested. Figure 3-21(c) is not an optimal configuration because of the proximity of placing a saturable absorber at sections 18 & 19. The high photon density from the HRC will make it difficult for the saturable absorber to recover and thus the laser would lose mode-locking. Figure 3-21(d) is not tested because of the fact that there are four sections of saturable absorber ($>750\text{-}\mu\text{m}$) and when this occurs mode-locking is lost and the device runs in c.w. The optimal condition was when section 14 and sections 9 and 10 were used as the saturable absorbers as seen in Figure 3-22. The data corresponding to this configuration is discussed in the following section.

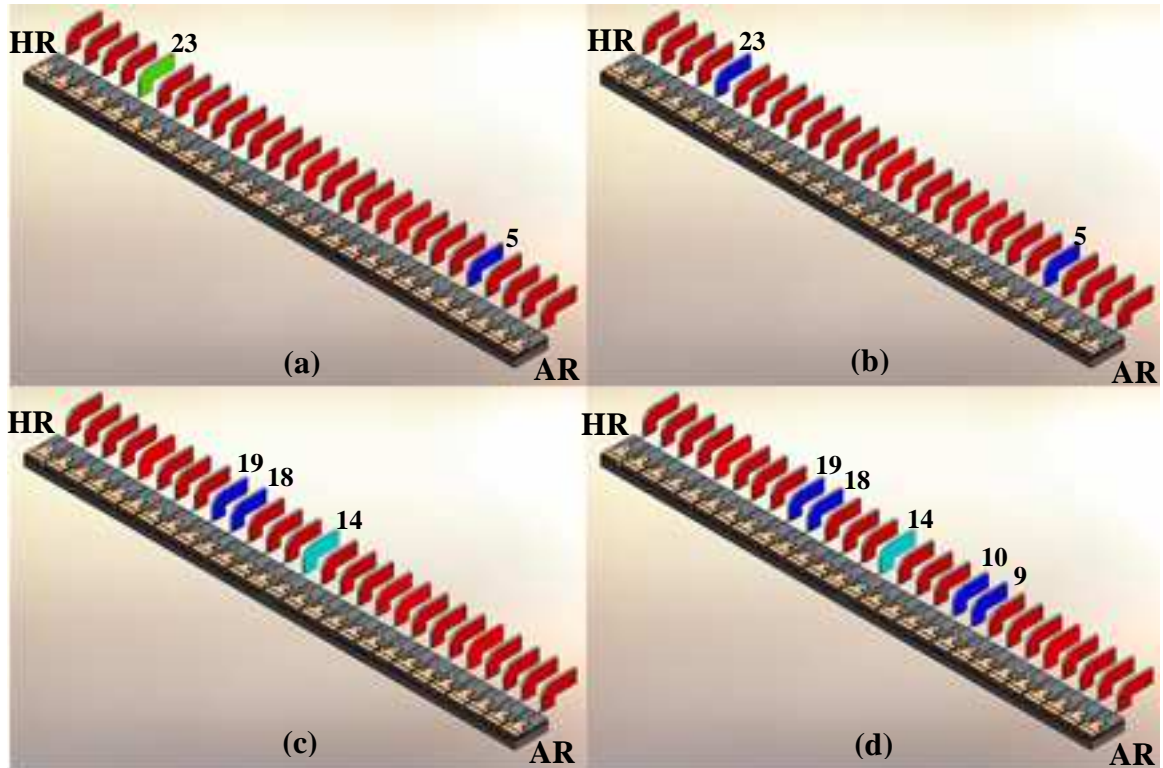


Figure 3-21 Possible configuration for the generation of the sixth harmonic. (a) Using the traditional method and placing a saturable absorber at either section 5 or 23, (b) using both sections 5 and 23, (c) using the double-interval technique by placing saturable absorbers at section 14 and 18&19, and (d) using the double-interval technique by placing saturable absorbers at section 14 and 9&10 and 18&19

Optimal Double-Interval Sixth Harmonic Configuration and Laser Characteristics

The double interval technique would stimulate the second and third harmonics concurrently to get their multiplicative value of six. This would correspond to placing a reverse bias at section 14 to simulate the second harmonic and placing a reverse bias on sections 18 and 19 and/or sections 10 and 9 in order to stimulate the third harmonics. As discussed earlier, placing a saturable absorber section beyond section 14 is of no use because it is desired to have the additional anti-node located next to the outputting facet. The sixth harmonic was stimulated when section 14 and sections 9 and 10 were used as the saturable absorbers as seen in Figure 3-22. Section 14 was biased with a reverse

voltage of 2.14 Volts, as indicated by the light blue probe, while sections 9 and 10 received a voltage of 0.00 Volts, as shown with the blue probes. The remainder of the laser diode was uniformly pumped with 300 mA (1111.11 A/cm^2), as shown with the red probes. The device is being more aggressively pumped because of the locations of the absorbers and the fact that there are three of them. The absorbers are closer to the ARC facet than before and the gain needed in order to saturate the absorber must be achieved by the increase in pumping current. Also, the increase of pumping current helps provide the gain needed to maintain the minimum of 0 dBm of average power needed to carry out the experiment. Figure 3-23 shows the sixth harmonic's repetition rate of the laser across a 50 GHz span and Figure 3-24 shows a 100 MHz span of the sixth harmonic's repetition frequency. It is apparent from Figure 3-24 that mode-locking is becoming more difficult to achieve. The configuration hardly meets the 15 dBm difference between the noise floor and the peak of the ESA measurement requirement for mode-locking decided upon before the experimentation. In essence it is becoming difficult for the laser to mode-lock. As shown in the figures, the sixth harmonic frequency for this laser is 36.120 GHz. Figure 3-25 shows the pulse width associated with the sixth harmonic having a FWHM of 6.82 ps.

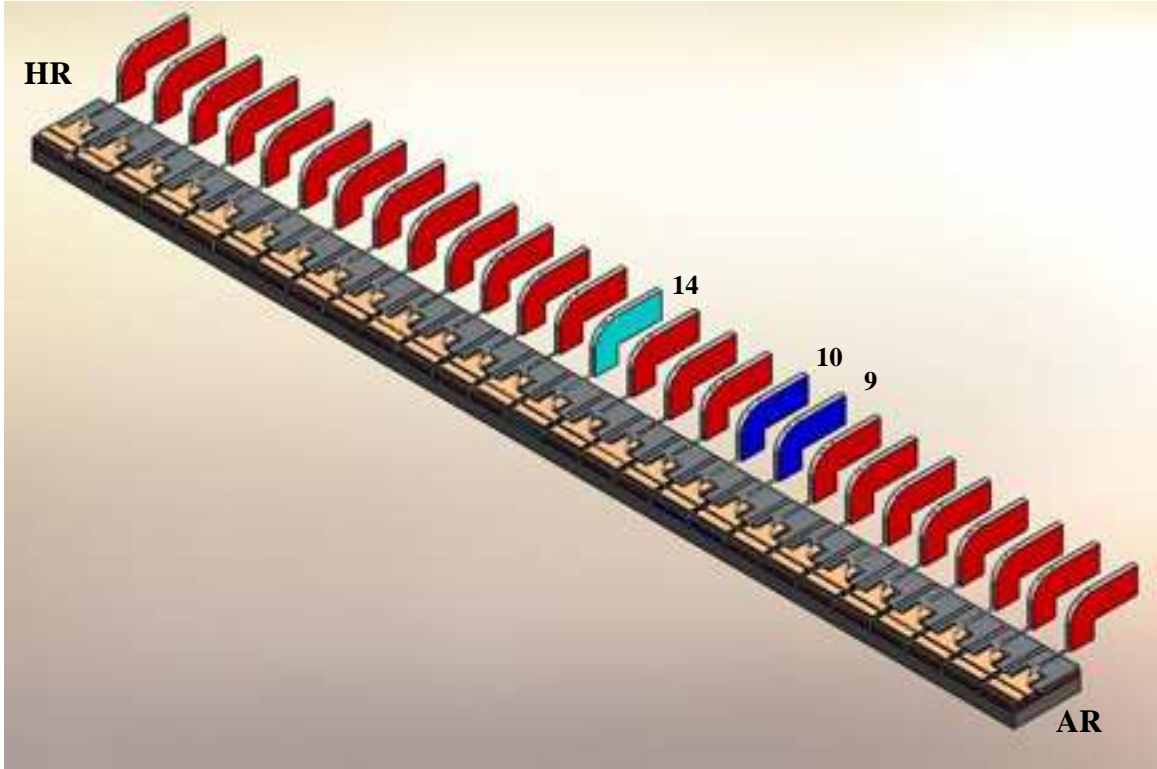


Figure 3-22 Double interval configuration for the generation of the sixth harmonic

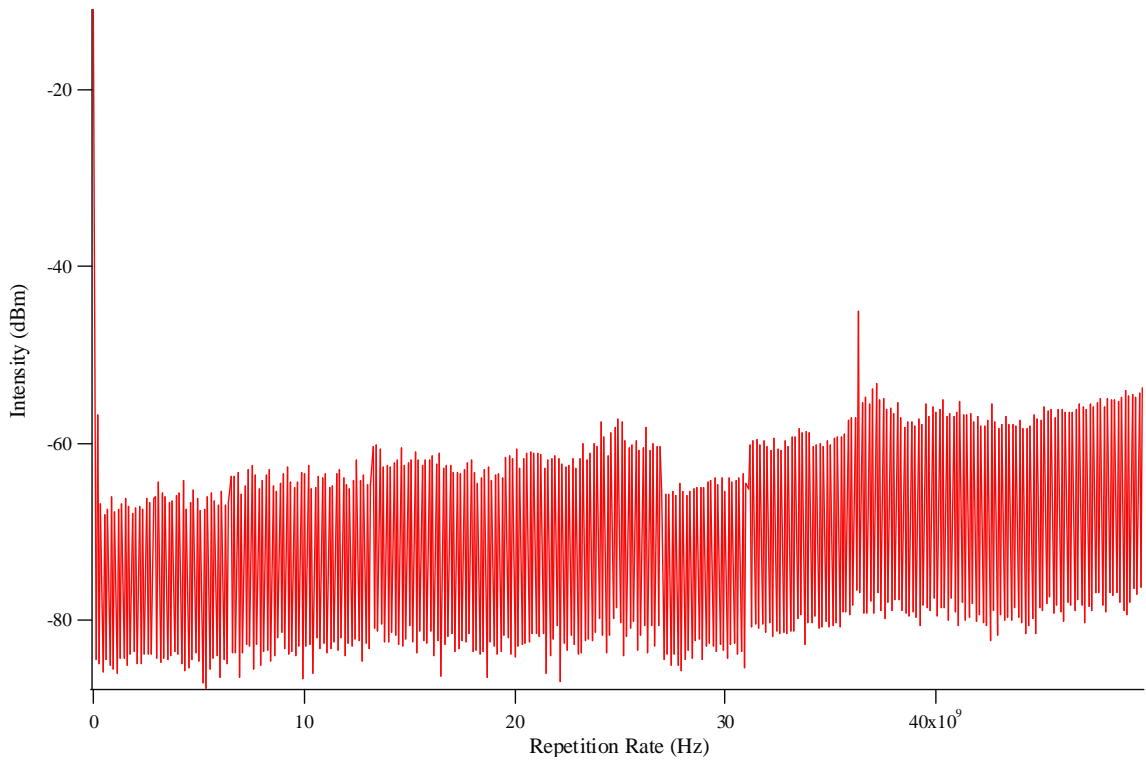


Figure 3-23 50 GHz Span of repetition rate while configured for sixth harmonic generation

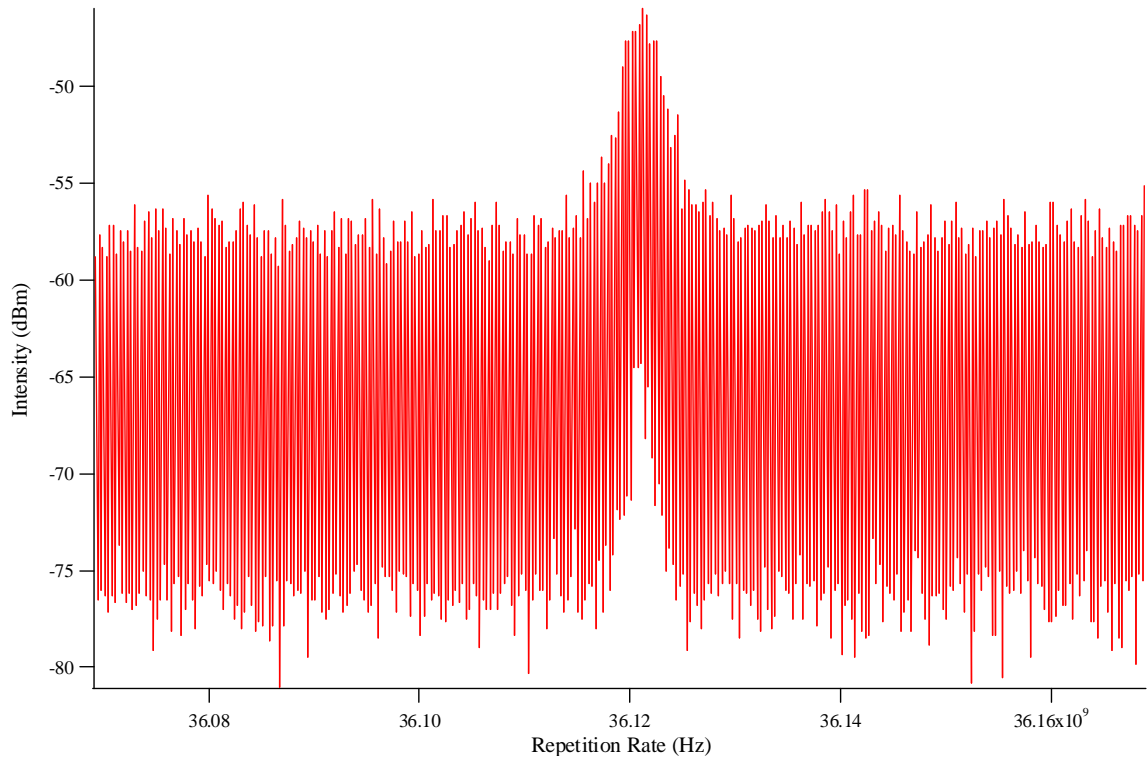


Figure 3-24 100 MHz span of the sixth harmonic repetition rate

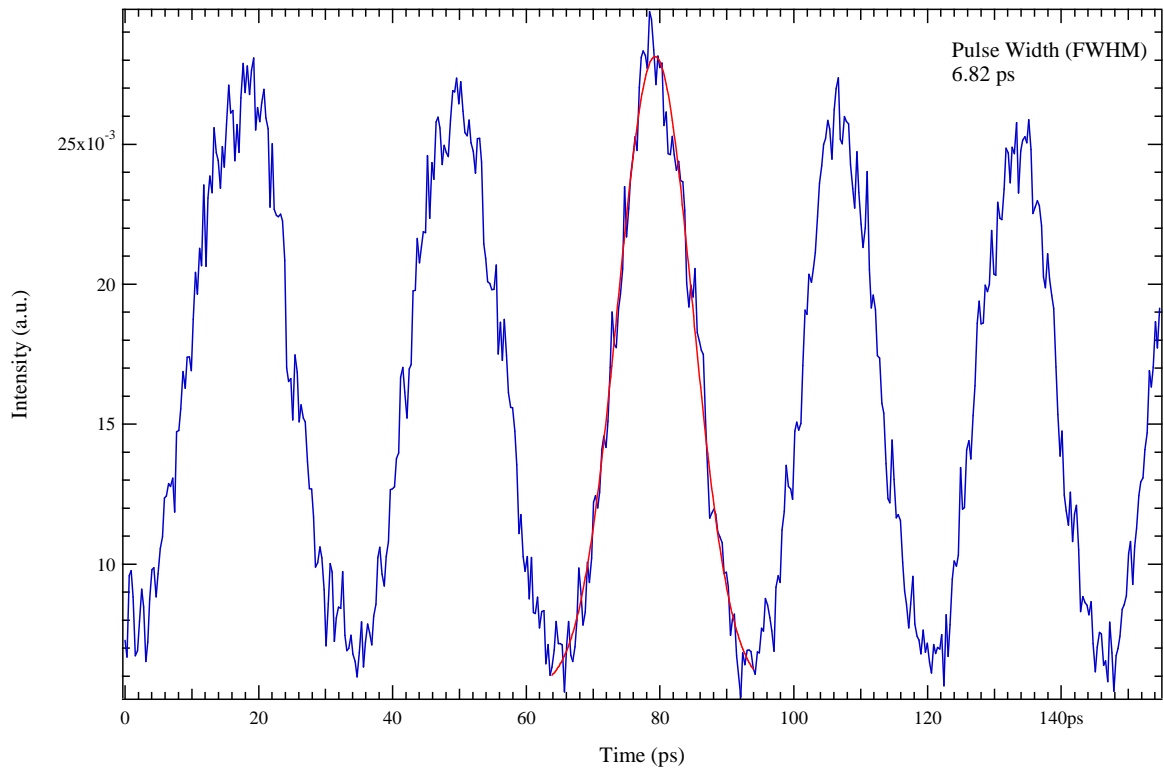


Figure 3-25 Pulse width associated with the sixth harmonic repetition rate

3.2.2 Tenth Harmonic Laser Characteristics

To mode-lock at a repetition rate that is the tenth harmonic, the saturable absorber could be placed at a location approximately one tenth of the laser's total length from either facet. Again, this could be impractical depending upon the laser's length and patterned segmentation. Figure 3-26(a) and Figure 3-26(b) show the configurations for stimulating the tenth harmonic using the traditional method. Using the traditional method, it becomes difficult to stimulate just the tenth harmonic by placing a saturable absorber at section 3 and/or 25. Due to the section size and laser length, an ambiguity occurs as the device is divided to correspond to higher harmonics. If a saturable absorber was placed at section 3 or 25, by geometry, it is difficult to know if this would stimulate just the tenth harmonic. Those absorber locations could also work for 9th – 13th harmonics because their desired midpoints lie within those sections. Thus the configurations in Figure 3-26(a) and Figure 3-26(b) are not considered. Since it has been shown that the second and fifth harmonics are possible, the double interval technique can be used to stimulate the tenth harmonic. The double interval technique would stimulate the second and fifth harmonics concurrently to get their multiplicative value of ten. This would correspond to placing a reverse bias at section 14 to simulate the second harmonic and placing another reverse bias at section 22 and/or section 6 in order to stimulate the fifth harmonic. Figure 3-26(c) shows the configuration corresponding to placing saturable absorbers at section 14 and section 22. Since the device will be pumped harder, placing a saturable absorber at section 22 is too close to the HRC. The high density of photons will constantly saturate the absorber and it will not be able to recover at all. This

would cause the device to lose mode-locking and thus run in c.w. Figure 3-26(d) shows the configuration corresponding to placing saturable absorbers at section 14, section 22, and section 6. Again section 22 is too close to the HRC and it would be difficult to mode-lock the device. The optimal condition was achieved when section 14 and section 6 were used as the saturable absorbers is seen in Figure 3-27. The data for this configuration will be discussed in the next section.

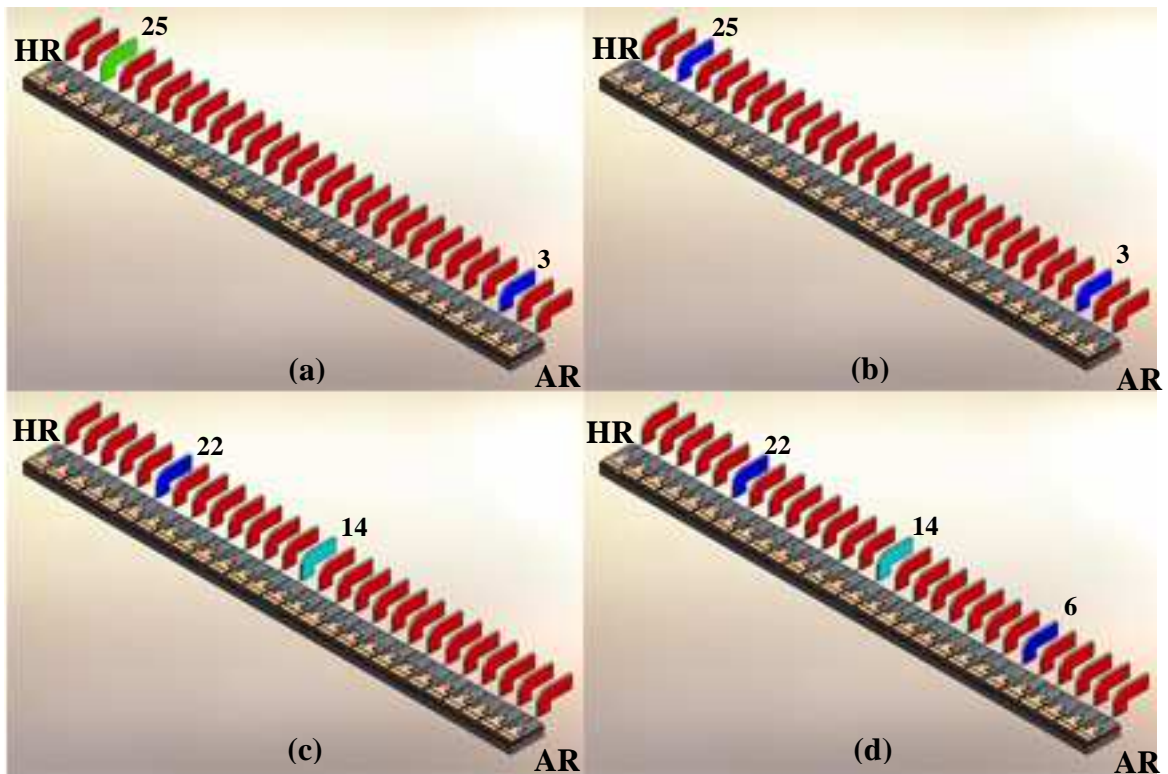


Figure 3-26 Possible configuration for the generation of the tenth harmonic. (a) Using the traditional method and placing a saturable absorber at either section 3 or 25, (b) using both sections 3 and 25, (c) using the double-interval technique by placing saturable absorbers at section 14 and 22, and (d) using the double-interval technique by placing saturable absorbers at section 14 and 6 and 22

Optimal Double-Interval Tenth Harmonic Configuration and Laser Characteristics

The tenth harmonic was achieved when section 14 and section 6 were used as the saturable absorbers is seen in Figure 3-27. Section 14 was biased with a reverse voltage of 0.10 Volts, as indicated by the light blue probe, while section 6 received a voltage of 4.72 Volts, as shown by the blue probe. For this case the device was no longer uniformly pumped across the remaining sections. Sections 1-5 were pumped with 62.0 mA (12.4 mA / 250- μ m section) as show in Figure 3-27 by the golden probes. The remaining sections (7-13 and 15-27) were pumped 280.0 mA total (14.0 mA / 250- μ m section), as shown by the red probes. Again due to the reverse bias voltages and the locations of the saturable absorbers, the current densities have been adjusted to satisfy the mode-locking conditions. Figure 3-28 shows the tenth harmonic's repetition rate of the laser across a 50 GHz span. This clearly demonstrates that the frequency is out of the range of the 45GHz photodetector. Figure 3-29 shows the pulse width associated with the tenth harmonic with a FWHM of 6.51 ps. Using the time interval and the number of pulses it is possible to estimate the laser's repetition rate. From Figure 3-29 the number of pulses (# pulses) is 12, and the ΔT is 203 ps. Solving $f_{rep} = \frac{\# \text{ pulses}}{\Delta T}$ the repetition rate is estimated to be

59.113 GHz ~ 60.0 GHz.

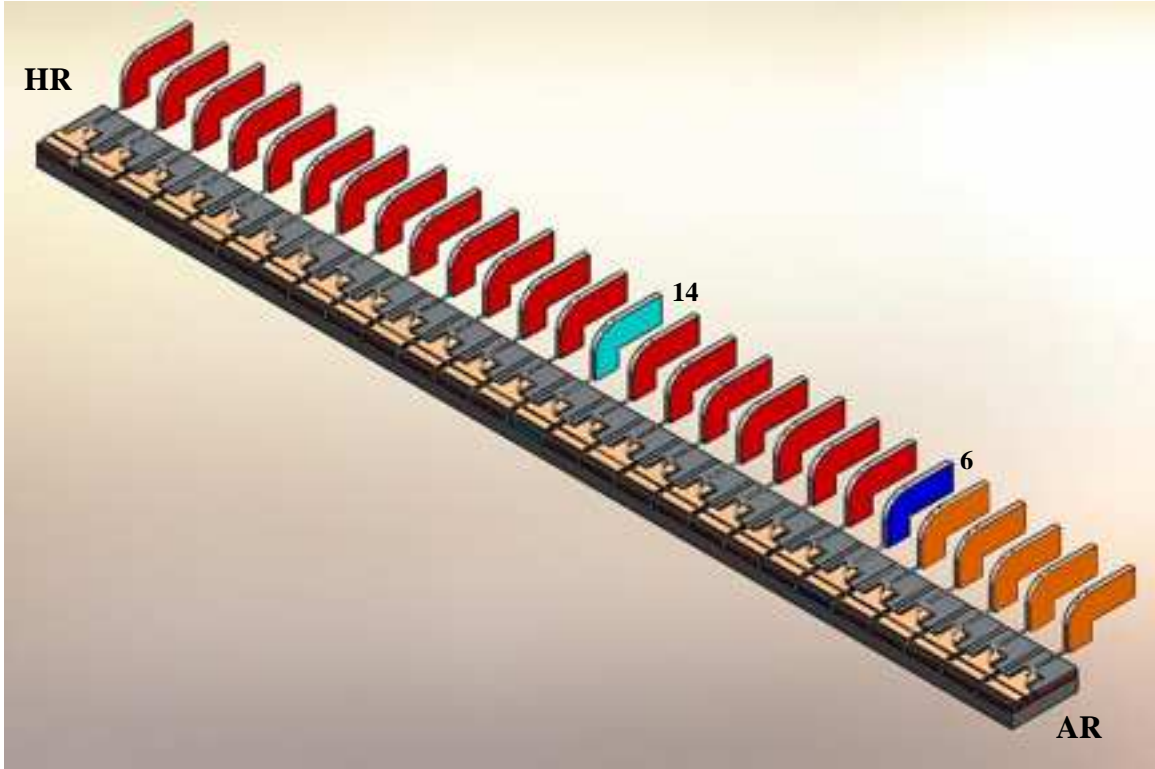


Figure 3-27 Double interval configuration for the generation of the tenth harmonic

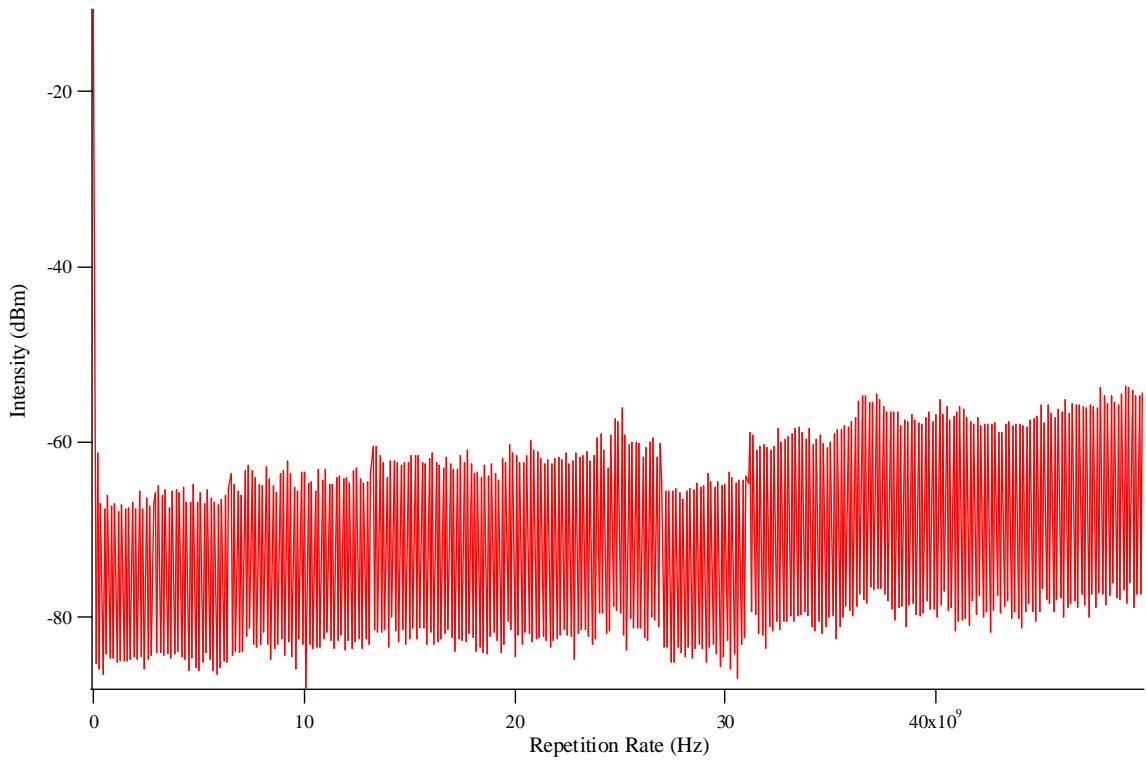


Figure 3-28 50 GHz span of repetition rate while configured for tenth harmonic generation

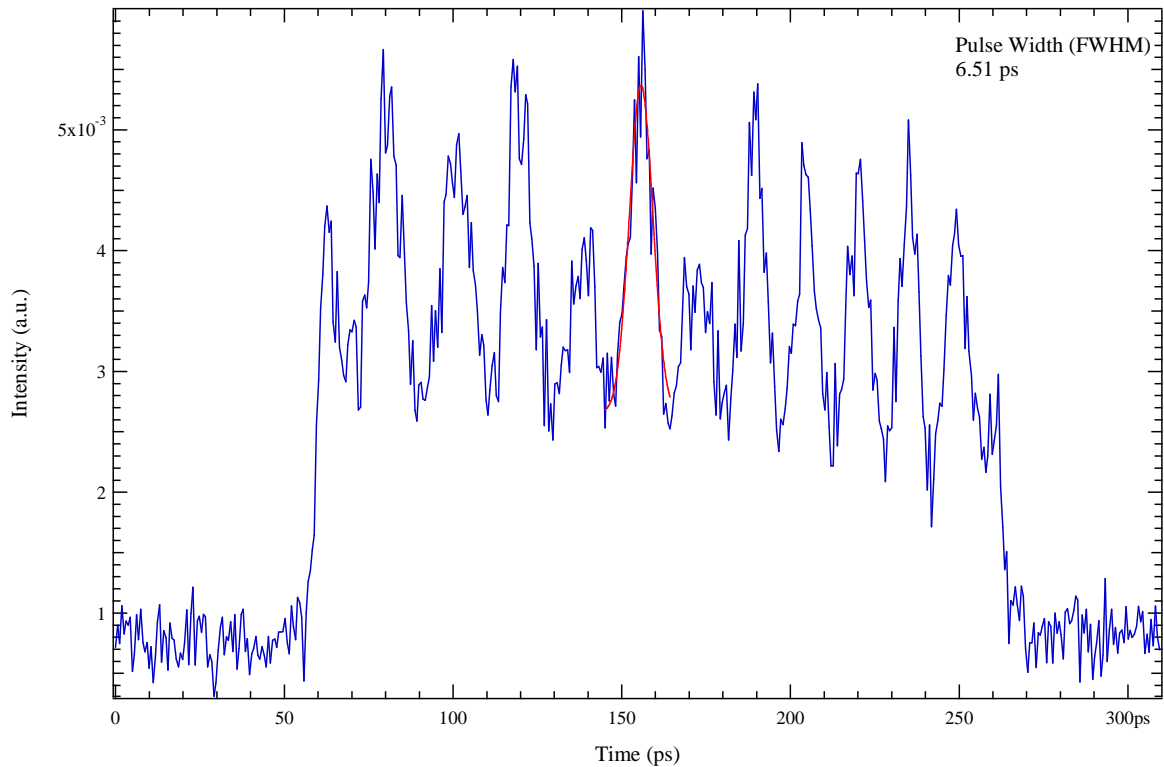


Figure 3-29 Pulse width associated with the tenth harmonic repetition rate

3.3 Analysis

As seen in the data, the higher order harmonics did correspond nicely to the expected values. The fundamental repetition rate of 6.019 GHz and the second, third, fifth, sixth, and tenth harmonics had repetition rates of 12.027 GHz, 18.023 GHz, 30.125 GHz, and 36.120 GHz, and 59.113 GHz, respectively. Since the device was divided up into 27 sections it was difficult to achieve perfect multiples of the fundamental harmonic. But it is the versatility of the double interval techniques and the device's geometry that made higher order harmonic stimulation possible. A comparison between the predicted values and the measured values can be seen in Table 3-1.

Harmonic to be Stimulated	Predicted Repetition Rate	Measured Repetition Rate
Fundamental	---	6.019 GHz
Second	12.038 GHz	12.027 GHz
Third	18.057 GHz	18.023 GHz
Fifth	30.095 GHz	30.125 GHz
Sixth	36.114 GHz	36.120 GHz
Tenth	60.190 GHz	59.113 GHz

Table 3-1 Comparison of expected values for the repetition rates and the measured values for the repetition rates for the harmonics generated

As different harmonics were stimulated the pulse widths changed as well. The smallest pulse width was produced when the third harmonic was stimulated. This is because of the fact that the mid-point of the absorber was exactly at the desired symmetry location. Also, there is a greater symmetric region of saturable absorber surrounding the midpoint allowing for pulse trimming. When the double interval technique was applied, the resultant pulse width was in between the pulse widths associated to the harmonics that were simultaneously stimulated. It is important to note that for the tenth harmonic the pulses are beginning to overlap and appear to be more comb-like rather than clearly defined. This is due to the fact that the laser is partially mode-locked and the pulses are occurring closer together.

Harmonic Stimulated	Pulse Width (ps)
Fundamental	4.96
Second	7.28
Third	4.34
Fifth	4.96
Sixth	6.82
Tenth	6.51

Table 3-2 Comparison between pulse widths and stimulated harmonics

CHAPTER 4 - SUMMARY AND FUTURE WORK

4.1 Summary

The objective of this thesis was to investigate higher order harmonic generation using the double interval technique of a passively locked mode-locked laser. While the double interval technique is not the only technique used to create mode-lock lasers, it provides the ability to create repetition rates that would not be easily achieved. It overcomes the difficulty of dividing a laser diode into infinitesimal sections by providing the ability to divide it into its multiplicative components. One goal of this experiment was to study a mode-locked laser and be able to control its harmonic generation. An additional goal was to use the double-interval technique to stimulate higher order. While it is possible to manufacture multiple lasers for multiple repetition rates, creating a laser that can be easily reconfigurable is highly desired.

The device used in this project is a 6.75-mm long GaAs semiconductor laser diode which was divided up into 27 250- μm sections. The laser was grown with 10 stacks of quantum dots (QD) to provide increased gain within the device. The saturable absorber was selected depending upon the harmonic to be stimulated. The absorber received a reverse bias voltage and was the location for the pulse collisions. The remaining sections of the laser diode were pumped with the necessary current density in order to stimulate the harmonic.

The stimulation of the first, second, third, fifth, sixth, and tenth harmonics was achieved in this thesis. The laser diode had a fundamental frequency of 6.019 GHz and a pulse width of approximately 4.96 ps. As expected, the frequencies for the second, third, fifth, sixth, and tenth harmonics were approximately the desired values. They were 12.027 GHz, 18.023 GHz, 30.125 GHz, 36.129 GHz, and 59.113 GHz, respectively.

4.2 Future Work

An area of interest is to combine the higher order harmonic generation with pulse compression techniques to achieve better defined pulses. As shown in Chapter 3, when the higher order harmonics are stimulated pulse widths begin to overlap. This overlapping can make it difficult to differentiate between pulses. In essence, the noise floor between pulses increases making the autocorrelation appear to be more comb-like rather than having distinctly defined pulses. With conventional pulse compression techniques, such as adding optical fiber with negative dispersion, it is possible to prevent the overlapping and create well defined pulses. This is advantageous because not only are the pulses well defined, but their pulse widths may be reduced as well. Another possible initiative would be the implementation of a harmonic crystal. This may provide the ability to create another multiple of the repetition rate exiting the laser. Another area of interest would be to see how the numbers of QD stacks affect mode-locking of the device. Since QDs have a tradeoff between gain and spectral width, it would be interesting to see how increasing the number of the QD stacks would affect the quality of the mode-locking. Also, the use of different length laser diodes would provide different fundamental repetition rates allowing for a vast range of frequencies. Alternatively, the

device could be segmented differently by creating a mask with 100- μm sections so the device could be divided up into even smaller sections for harmonic stimulation. This would allow for even more segmentation of the device and thus allowing for higher harmonics.

REFERENCES

- [1] L.Zhang, L.Cheng, A.L.Gray, S.Luong, J.Nagyvary, F.Nabulsi, L.Olona, K.Su, T.Tumolillo, R Wang, C.Wiggins, J.Ziko, Z.Zau, P.M.Varangis, Su, H., and Lester, L. F., "5 GHz Optical Pulses From a Monolithic Two-Section Passively Mode-locked 1250/1310 nm Quantum Dot Laser for High Speed Optical Interconnects," *Optical Fiber Communication Conference.Technical Digest.OFC/NFOEC*, vol. 3, 6-11 2005.
- [2] Gaburro, Z., "Optical interconnect", in *Silicon Photonics*; 2004; Vol.94, pp.121-176, Pavese L & Lockwood, D. J., *Topics in Applied Physics*, Springer Verlag, 2004.
- [3] Derickson, Dennis J., Helkey, Roger J., Mar, Alan, Karin, Judy R., Wasserbauer, John G., Bowers, John G., "Short Pulse Generation Using Multisegment Mode-Locked Semiconductor Laser", *IEEE Journal of Quantum Electronics*, vol. 28, no. 10, pp. 2186-2202, October 1992.
- [4] A. Gubenko, D. Livshits, I. Krestnikov, S. Mikhrin, A. Kozhukhov, A. Kovsh, N. Ledentsov, A. Zhukov, E. Portnoi, "High-power monolithic passively modelocked quantum-dot laser", *Electronics Letters*, vol. 41, no. 20, September 2005.
- [5] Avrutin, Eugene A., Marsh, John H., J. M. Arnold, T. F. Krauss, H. Pottinger, R.M. De La Rue, "Analysis of harmonic (sub) THz passive mode-locking in monolithic compound cavity Fabry-Perot and ring laser diodes", *IEE Proceedings – Optoelectronics*, Vol. 146, no. 1, February 1999.

- [6] Yanson, Dan A., Street, Michael W., Avrutin, Eugene A., McDougall, Stewart D., Thayne, Iain G., Marsh, John H., “Passive harmonic modelocking in monolithic compound-cavity laser diodes”, *Electronics Letters*, vol. 36, no. 23, November 2000.
- [7] F. Camacho, Avrutin, Eugene A., P. Cusumano, A. Saher Helmy, A. C. Bryce, Marsh, John H., “Improvements in Mode-Locked Semiconductor Diode Lasers Using Monolithically Integrated Passive Waveguides Made by Quantum-Well Intermixing”, *IEEE Photonics Technology Letters*, vol. 9, no. 9, September 1997.
- [8] Kärtner, Franz, Ultra Fast Optics MIT Online Course 6.977, Spring 2005.
- [9] Huggett, George, R., “Mode-Locking of CW Lasers by Regenerative RF Feedback”, *Applied Physics Letters*, vol. 13, no. 5, September 1968.
- [10] Vasil’ev, Peter, *Ultrafast Diode Lasers Fundamentals and Applications*, Boston: Artech House 1995.
- [11] Encyclopedia of Laser Physics and Technology, *Active Mode-Locking*, http://www.rp-photonics.com/active_mode_locking.html.
- [12] Encyclopedia of Laser Physics and Technology, *Passive Mode-Locking*, http://www.rp-photonics.com/passive_mode_locking.html.
- [13] Verdeyen, Joseph T., *Laser Electronics*, 3rd edition, 1995.
- [14] Siegman, Anthony E., *Lasers*, Mill Valley, CA: University Science Books, 1986, Ch.27.

- [15] Valdmanis, J. A., R. L. Fork, and J. P. Gordon, "Generation of Optical Pulses as Short as 27 fs Directly from a Laser Balancing Self-Phase Modulation, Group Velocity Dispersion, Saturable Absorption, and Saturable Gain", *Optics Letters*, Vol. 10, 1985, pp. 131-133.
- [16] Yanson, Dan A., Street, Michael W., McDougall, Stewart D., Thayne, Iain G., Marsh, John H., Avrutin, Eugene A., "Ultrafast Harmonic Mode-Locking of Monolithic Compound-Cavity Laser Diodes Incorporating Photonic-Bandgap Reflectors", *IEEE Journal of Quantum Electronics*, Vol. 38, No. 1, January 2002.
- [17] Bischoff, S., Mork, J., Franck, T., Brorson, S. D., Hofmann, M., Frojdg, K., Prip, L., and Sorensen, M. P., "Monolithic colliding pulse mode-locked semiconductor lasers," *Quantum and Semiclassical Optics*, Vol. 9, No.5, pp. 655-674, 1997.
- [18] Shimizu, T., Wang, X. L., and Yokoyama, H., "Asymmetric colliding-pulse modelocking in InGaAsP semiconductor lasers," *Optical Review*, vol. 2, no. 6, pp. 401-403, 1995.
- [19] Shimizu, T., Ogura, I., and Yokoyama, H., "860 GHz rate asymmetric colliding pulse modelocked diode lasers," *Electronics Letters*, vol. 33, no. 22, pp. 1868-1869, 1997.
- [20] H. A. Haus, "Mode-locking of lasers," *IEEE J. Sel. Top. Quantum Electron.* 6, 1173-1185 (2000).

[21] "Illustration of harmonic overtones on the wave set up along a string when it is held steady in certain places, as when a guitar string is plucked while lightly held exactly half way along its length."

http://en.wikipedia.org/wiki/Image:Harmonic_partials_on_strings.svg

[22] H. A. Haus and Y. Silberberg, "Theory of mode-locking of a Laser Diode with a multiple-quantum-well structure," *J. Opt. Soc. Am. B* 2, 1237-1243 (1985).

[23] G. New, "Pulse evolution in mode-locked quasi-continuous lasers," *IEEE J. Quantum Electron.* 10, 115-124 (1974).

[24] E. A. Viktorov, P. Mandel, A. G. Vladimirov, and U. Bandelow, "Model for mode locking in quantum dot lasers," *Appl. Phys. Lett.* 88, 201102 (2006).

[25] F. Lelarge, B. Dagens, J. Renaudier, R. Brenot, A. Accard, F. van Dijk, D. Make, O. Le Gouezigou, J. G. Provost, F. Poingt, J. Landreau, O. Drisse, E. Derouin, B. Rousseau, F. Pommereau, and G. H. Duan, "Recent advances on InAs/InP quantum dash based, semiconductor lasers and optical amplifiers operating at 1.55 μm ," *IEEE J. Sel. Top. Quantum Electron.* 13, 111-124 (2007).

[26] K. Y. Lau and J. Paslaski, "Condition for short pulse generation in ultrahigh frequency mode-locking of Semiconductor-Lasers," *IEEE Photon. Technol. Lett.* 3, 974-976 (1991).

[27] J. Paslaski and K. Y. Lau, "Parameter ranges for ultrahigh frequency mode-locking of semiconductorlasers," *Appl. Phys. Lett.* 59, 7-9 (1991).

- [28] H. Haus, "Parameter ranges for CW passive mode locking," *IEEE J. Quantum Electron.* 12, 169-176 (1976).
- [29] Abraham NB, Huang JC, Kranz DA, Rockower EB, "Amplified-Spontaneous-Emission Intensity Fluctuations", *Physical Review A* , v. 24(5) pp. 2556 1981
- [30] Joseph T.Verdeyen, *Laser Electronics 3rd Edition*, 1995 Prentice Hall Professional Technical Reference, New Jersey.
- [31]Oster, A; Erbert, G; Wenzel, H, "Gain spectra measurements by a variable stripe length method with current injection", *Electronics Letters* 33, 864-866, 1997
- [32] Yongchun Xin. Quantum Dot Multi-Section Light Emitters. Dissertation, University of New Mexico, Albuquerque, 2006.
- [33] D. J. Derickson, R. J. Helkey, A. Mar, J. R. Karin, J. G. Wasserbauer, and J. E. Bowers, "Short pulse generation using Multisegment Mode-Locked Semiconductor-Lasers," *IEEE J. Quantum Electron.* 28, 2186-2202 (1992).